

Integrated approach to assess the environmental impact of mining activities: estimation of the spatial distribution of soil contamination (Panasqueira mining area, Central Portugal)

Carla Candeias · Paula F. Ávila ·
Eduardo Ferreira da Silva · João Paulo Teixeira

Received: 19 February 2014 / Accepted: 9 February 2015 / Published online: 22 February 2015
© Springer International Publishing Switzerland 2015

Abstract Through the years, mining and beneficiation processes in Panasqueira Sn-W mine (Central Portugal) produced large amounts of As-rich mine wastes laid up in huge tailings and open-air impoundments (Barroca Grande and Rio tailings) that are the main source of pollution in the surrounding area once they are exposed to the weathering conditions leading to the formation of acid mine drainage (AMD) and consequently to the contamination of the surrounding environments, particularly soils. The active mine started the exploration during the nineteenth century. This study aims to look at the extension of the soil pollution due to mining activities and tailing erosion by combining data on the degree of soil contamination that allows a better understanding of the dynamics inherent to leaching, transport, and accumulation of some potential toxic elements in soil and their environmental relevance. Soil samples

were collected in the surrounding soils of the mine, were digested in aqua regia, and were analyzed for 36 elements by inductively coupled plasma mass spectrometry (ICP-MS). Selected results are that (a) an association of elements like Ag, As, Bi, Cd, Cu, W, and Zn strongly correlated and controlled by the local sulfide mineralization geochemical signature was revealed; (b) the global area discloses significant concentrations of As, Bi, Cd, and W linked to the exchangeable and acid-soluble bearing phases; and (c) wind promotes the mechanical dispersion of the rejected materials, from the milled waste rocks and the mineral processing plant, with subsequent deposition on soils and waters. Arsenic- and sulfide-related heavy metals (such as Cu and Cd) are associated to the fine materials that are transported in suspension by surface waters or associated to the acidic waters, draining these sites and contaminating the local soils. Part of this fraction, especially for As, Cd, and Cu, is temporally retained in solid phases by precipitation of soluble secondary minerals (through the precipitation of hydrated metal sulfates) in warm, dry periods, but such minerals are easily dissolved during rainy periods. Climate is an important instability factor, and the hot and dry summers and cold, rainy, and windy winters in this region are physical phenomena that enhance the good receptivity of these soils to retain some of the metals present in the primary and also the secondary mineralogy. Considering the obtained results from both the sequential chemical extraction and the environmental risk assessment according to the risk assessment code, Ag, Cd, Cu, and Zn are classified with very high risk while As is classified with medium risk.

C. Candeias (✉) · E. Ferreira da Silva
GeoBioTec—Geobiosciences, Geotechnologies e
Geoengineering Research Center, Geosciences Department,
University of Aveiro, Campus de Santiago, 3810-193 Aveiro,
Portugal
e-mail: candeias@ua.pt

P. F. Ávila
LNEG—National Laboratory of Energy and Geology, S.
Mamede de Infesta, Rua da Amieira, Apartado 1089,
4466-901 S. Mamede de Infesta, Portugal

J. P. Teixeira
Environmental Health Department, National Institute of
Health, Rua Alexandre Herculano, 321, 4000-055 Porto,
Portugal

Keywords Soil · Principal component analysis · Geostatistics · Environmental geochemistry · Panasqueira mine

Introduction

Modern mining is an industry that involves the exploration and removal of minerals from the earth, economically and with minimum damage to the environment. It is known that mining industry may cause negative impacts in its surrounding areas. Operations, whether in small or large scale, are inherently disruptive to the environment, producing enormous quantities of wastes that can have deleterious impacts for decades (Fernandes-Caliani et al. 2009). The environmental deterioration caused by mining activities occurs mainly as a result of inappropriate and wasteful working practices. Mining operations routinely modify the surrounding landscape by exposing previously undisturbed earthen materials. Erosion of exposed soils, extracted mineral ores, tailings, and fine material in waste rock piles can result in substantial sediment loadings to surface waters and drainage routes. In addition, spills and leaks of hazardous materials and the deposition of contaminated windblown dusts can lead also to soil contamination.

The consequences can become particularly worrying whenever the exploitation and ore treatment operations are performed in the vicinity of villages. Soils and waters can be easily contaminated by metals/metalloids due to their direct contact (and interference) with the chemical processes of metal liberation and mobilization that commonly results from mining operations (Kabata-Pendias 2011). Mine wastes containing high sulfide concentrations are among the most serious sources of environmental pollution. Understanding the geochemical processes which control precipitation and dissolution of secondary minerals in abandoned sulfide mines is crucial for the elaboration of models which predict the environmental impact of such sites (Moncur et al. 2009).

Soil is not only a part of the ecosystem but also plays a basic role for humans, because the survival of man is tied to the maintenance of its productivity (Kabata-Pendias and Mukherjee 2007). Human health and environmental risks from soils generally fall into two categories: (1) soil contaminated from chemical spills and residues and (2) contaminated soil resulting from wind-blown dust. Soils contaminated from chemical spills and residues at mine sites may pose a direct contact risk

when these materials are misused as fill materials, ornamental landscaping, or soil supplements.

Fugitive dust can pose significant environmental problems at some mines. Tailings in particular can be a strong source of fine particulates. The inherent toxicity of the dust depends upon the proximity of environmental receptors and type of ore being mined. High levels of As, Pb, and radionuclides in windblown dust usually pose the greatest risk.

The long history of exploitation and ore treatment operations in the Panasqueira mine are testified by the presence of huge tailings and other debris. The rejected materials can be classified as coarse materials, coarse slag, sand, and mud. The first three are disposed on tailings while muds (some rich in sulfides) are dropped on dams built specifically for that proposal (e-Ecorisk 2007). First, these materials were disposed in the Vale de Ermida (~100,000 m³). The site is characterized by the presence of old infrastructures as well as large tailing piles from the earliest years of production (late 1895 to 1928; Leal 1945) that were abandoned when the new plant was constructed at Rio (Leal 1945). By that time, the ore was transported from Barroca Grande along a 5.1-km cableway further down the Zêzere River to the concentration plant located at Rio (formerly known as Cabeço do Pião). The waste materials from the mineral extraction and from the mineral milling processes have been disposed for approximately 100 years (historical records show that that started after 1901 and was deactivated in 1996). The Rio tailing site (~1,200,000 m³) and the open-air impoundment constructed in the top of the tailing (~731,034 m³) are located on the left bank of the Zêzere River. On the top of the Rio tailing, an arsenopyrite stockpile (~9400 m³) was deposited and remained exposed until June 2006 when it was capped with geotextile and layers of clay (e-Ecorisk 2007). Since 1996, offices, underground exploration, milling processes, and tailing (~7,000,000 m³) and mud dams (~1,193,885 m³; one active and one deactivated) are located in Barroca Grande. All these materials are exposed to the atmospheric conditions for a long time, which affect their chemical, mineralogical, physical, and geotechnical elements. The percolation of rainwaters is responsible by the dissolution of slags, forming acid mine drainage (AMD) causing serious damages on the surrounding environment (Ávila et al. 2008a).

The objectives of the present study are (1) to evaluate the extent of pollution in soils impacted by mining

activities and by erosion of the tailings, (2) to determine the associations between the different toxic elements and their spatial distribution, (3) to identify other possible sources of contamination that can explain the spatial patterns of soil pollution, and (4) to evaluate the anthropogenic and lithogenic contribution in soils.

Study area location and environmental settings

Geographical location and land use The studied area is located between Gardunha and S. Pedro de Açor Range Mountains. The Panasqueira mine is located geographically in the municipalities of Covilhã and Fundão (Castelo Branco district, Central Portugal). The work

site includes Barroca do Zêzere, S. Francisco de Assis, and S. Martinho municipalities, which belong to the Castelo Branco district, and also Dornelas do Zêzere municipality belonging to the Coimbra district (Fig. 1).

Topography ranges in altitude from 350 to 1080 m (Reis 1971), with deep valleys of about 9–25 % slope constraining the soils in to a very thin layer. Climate is severe, with dry and hot summers and very cold, rainy, and windy winters. The annual precipitation ranges between 1200 and 1400 mm with frequent snow falling, particularly above 700 m altitude. The mean annual temperature is 12 °C, ranging from 0 °C during the winter to 30 °C in the summer. The evapotranspiration in this region is around 1080 mm (data available in www.inag.pt, August 2011). The streams are generally

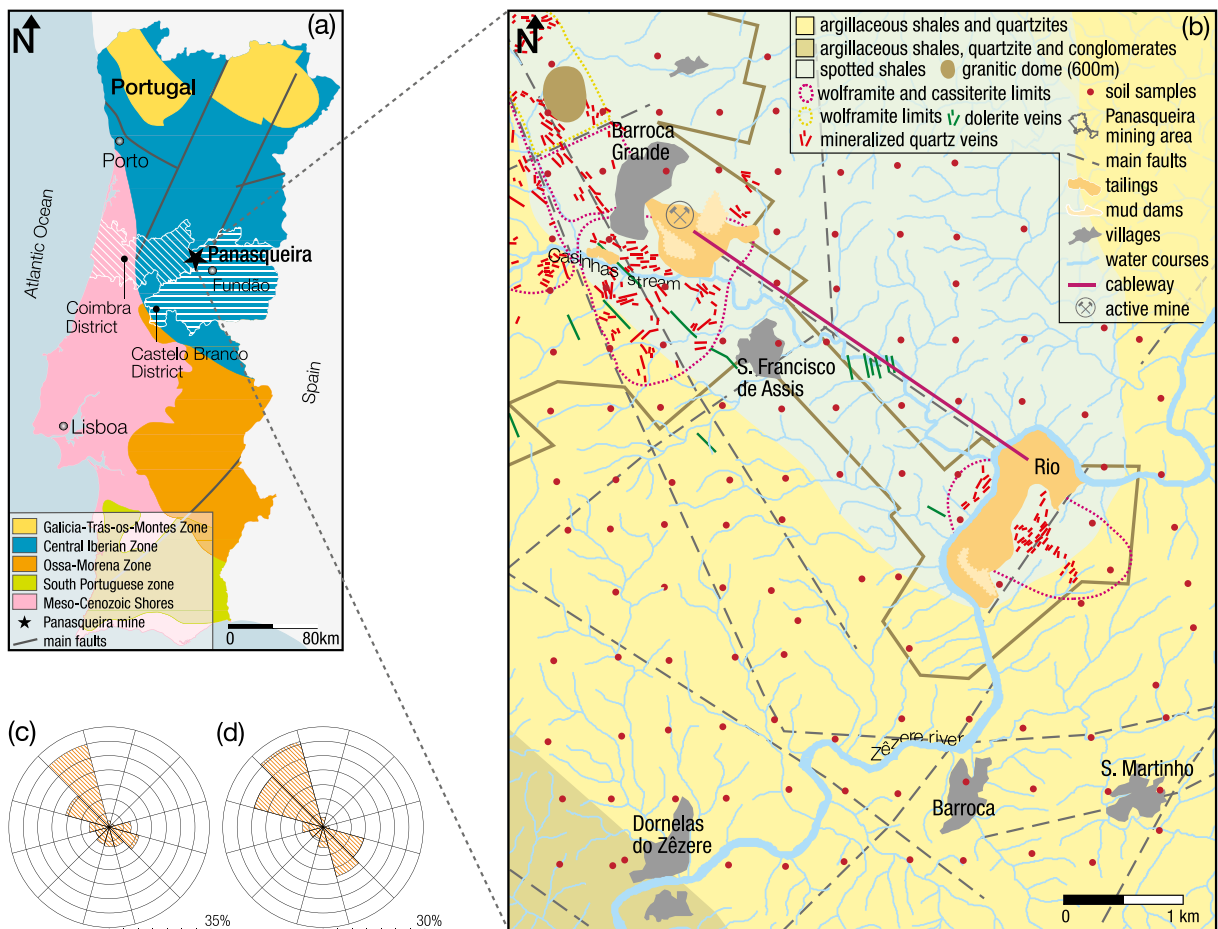


Fig. 1 a Synthetic map of Portugal showing the location of Panasqueira mining area; b detail of the study area, main geological units, and soil sample grid (geological map adapted from Jaques Ribeiro and Gonçalves (2013), e-Ecorisk (2007), and Thadeu (1951)); c wind rose of the prevailing winds on the top

of the mine (Barroca Grande tailing); and d on the top of a mountain 800 m north of the mine (extracted from CD-ROM “Atlas do Potencial Eólico para Portugal Continental, Version 1.0”)

dry in the summer and flooded in the winter. According to Costa and Estanqueiro (2006a, b) and Costa (2004), the prevailing wind in the area is NW-SE with mean wind speeds of 4.22 m/s ($h=10$ m), 5.55 m/s ($h=40$ m) and 6.21 m/s ($h=80$ m) (Fig. 1c, d). Vegetation (forest area ~60 %) consists mostly of broom plantation and heather, and also *Castanea sativa*, *Ulmus* L., *Eucaliptus globulus* Lab., *Quercus robur* L., and *Arbutus unedo*. Agricultural and urban areas are also important. The small villages around the mine have a historical dependence on soil and water use—drinking water, agriculture, cattle breeding, fishing, and forestry.

Geology According to the paleogeographic and tectonic zoning established by Julivert et al. (1974) and Lotze (1945), this deposit is included in the Central Iberian Zone (CIZ; Fig. 1). The Panasqueira deposit lies in a folded metasedimentary sequence known as the upper Precambrian-Cambrian aged Beira schist formation which is composed of a several thousand meter thick sequence of lower marine flyschoid schists, graywackes, lenticular, thinly bedded mudstones, shales, and arenites (Thadeu 1951).

The dominant lithological unit hosting the tungsten concessions of the Sojitz Beralt Tin & Wolfram Company is of Cambrian to Upper Cambrian age and forms an outcrop of about 35 km²; however, brown argillaceous schists and dark gray siliceous schists interbedded with rare graywackes were identified in the area. Few mafic rocks (dolerites) were observed, particularly near S. Jorge da Beira (NW-SE subvertical). Some quartz veins disposed parallel to the principal schistosity were also mapped.

Soil type According to Cardoso et al. (1971) Leptosols (eutric) are predominant in the study area, coexisting with Cambisols (humic). Leptosols show little soil formation processes which lead to a very shallow depth to hard bedrock. For this reason, these soils are very susceptible to erosion, desiccation, or waterlogging, especially in regions like Panasqueira, with very markedly topography and severe climatic conditions. Cambisols are characterized by a deficient layer of accumulated clay, humus, soluble salts, or Fe and Al oxides. These types of soils have at least 8 % clay and a minimum thickness of 15 cm.

Mineralization The Panasqueira ore deposit is a typical example of a Sn-W hydrothermal mineralization

associated with the Hercynian plutonism. The mineralized zone has an average length of 2500 m, ranges in width from 400 to 2200 m, and extends at least 500 m in depth (Cavey and Gunning 2006). The Panasqueira deposit consists of a series of stacked, sub-horizontal, hydrothermal quartz veins intruding into the Beira schists formation and shales. The paragenesis is complex; nevertheless, four stages of mineral formation are generally accepted by most of the authors who have studied this deposit: (1) oxide-silicate phase (quartz, wolframite, cassiterite), (2) main sulfide phase (pyrite, arsenopyrite, pyrrhotite, sphalerite, chalcocopyrite), (3) pyrrhotite alteration phase (marcasite, siderite, galena, Pb-Bi-Ag sulphosalts), and (4) late carbonate phase (dolomite, calcite) (Breiter 2001; Noronha et al. 1992). At Panasqueira, more than 65 minerals, including sulfides, sulphosalts, oxides, carbonates, silicates, phosphates, and tungsten minerals, have been identified (Kelly and Rye 1979). In general, the most common minerals in addition to quartz are wolframite, pyrite, pyrrhotite, arsenopyrite, chalcocopyrite, cassiterite, beryl, mica, and fluorite. Many of the other minerals are very rare and can only be observed microscopically. For example, native antimony was identified only once as an inclusion in a specimen of galena. Native gold and silver were noted together with pyrite and were detected in a silver and lead sulphosalt. Native bismuth has been found as inclusions in arsenopyrite and chalcocopyrite and is normally associated with bismuthinite, pavonite, or matildite

Mining activity Historical data shows that Romans worked the area for tin. According to Leal (1945), the first prospecting license was granted in 1898 and the first reference to wolframite mineralization in Panasqueira mine reportedly dated to 1888. The Panasqueira mining concession covers an area of more than 2000 ha and has been managed by a series of partnerships, with International and/or Portuguese companies, being actually known as “Sojitz Beralt Tin & Wolfram (Portugal) SA.” The mining activity had an accelerated expansion during World War I (WWI) and II (WWII). In both periods, the high demand for tungsten promoted that the local population had worked the superficial veins (approximately 1000 in WWI and 4800 in WWII) in the surrounding areas. The first underground drifts were opened at Panasqueira and Rio (Cabeço do Pião) sections, but mining activity decreased there as richer veins were discovered at the

Panasqueira site. The exploitation was extended to other areas, in 1928, the most important being Barroca Grande, Corga Seca, Alvoroso, and Vale das Freitas (Leal 1945). The economic exploitation has been mainly focused on wolframite, cassiterite, and chalcopyrite, the last two as by-products. On average, the “tout-venant” contains 0.3 % WO_3 and the three final concentrates are recovered with 75 % WO_3 , 72 % SnO_2 , and 22 % Cu together with significant amounts of Ag. At the present time, exploitation is focused at Barroca Grande with underground works that use the room and pillar mining methods. The Panasqueira mine has been in production for over 110 years and is one of the largest economic vein deposits in the world. During the period 1947–2001, the mine produced about 96,456 t of WO_3 , 4901 t of SnO_2 , and 28,924 t of Cu from more than 27 Mt of rock (Cavey and Gunning 2006).

Materials and methods

Field sampling

Rock samples Argillaceous shales (Sch_1 and Sch_2), spotted argillaceous shales (Sch_{sp}), quartzite (Qz), and spotted quartzite (Qz_{sp}) samples were collected from the study area. About 1 kg of each rock sample was crushed with a jaw crusher and pulverized in a mechanical agate mill. The samples were reduced to 250 g by coning and quartering, followed by drying at 40 °C. After homogenization, aliquots of 30–50 g of each dried sample were powdered in a mechanical agate mill.

Soil samples Soil samples were collected according to a defined grid (400 m × 400 m; Fig. 1b). Each sample was georeferenced and collected after clearing the soil surface of superficial debris and vegetation. Two types of soil samples were collected in each sampling site: 122 topsoil (0–15 cm) samples (Soil_0) and 116 subsurface soilsamples collected below 15-cm depth (Soil_{15}). The different number of samples is due to the presence of incipient and lithic soils derived from metasediment substrate, which turned impossible to collect six subsurface soil samples. Topsoil samples were collected aiming the characterization of superficial contamination coming from the tailings and subsurface soil samples to analyze the extent of the contamination in depth and simultaneously the attempt to identify the geogenic

markers. To establish the local geochemical background (B_k), 47 unaffected soil samples were also collected outside of the contaminated area (Casegas area located NE, out of the influence of the Barroca Grande prevailing winds). All the samples have been located by GPS and georeferenced with UTM coordinates. After collection in polyethylene bags, the samples were dried in an oven at 40 °C, homogenized, sieved (<2 mm) and pulverized to <170 μm in a mechanical agate mill for chemical analysis.

Chemical analysis

Rock samples The powdered rock samples were submitted for chemical analysis and multielement analysis to ACME (Anal. ISO 9002 Accredited Lab-Canada). For major and trace element analysis, a 0.25-g aliquot of each powdered sample was heated in $\text{HClO}_4\text{-HNO}_3\text{-HCl-HF}$ to fuming and taken to dryness (ACME; see <http://acmelab.com>). The residue was dissolved in HCl. The solution was analyzed by inductively coupled plasma atomic mass spectrometry (ICP-MS). The digestion is only partial for some S, Cr, and Ba minerals and some oxides of Al and Mn. Volatilization during fuming may result in some loss of As, Sb, and Au. The detection limits for trace elements were as follows: 0.1 mg kg^{-1} for Ag, Bi, Cd, Cu, La, Mo, Ni, Pb, Sb, Th, and W; 0.2 mg kg^{-1} for Co; 0.5 mg kg^{-1} for Te and Tl; 1 mg kg^{-1} for As, Ba, Cr, Mn, Sc, Se, Sr, and Zn; and 4 mg kg^{-1} for V. The detection limits for major elements were as follows: 0.01 g kg^{-1} for Na, P, and Ti; 0.1 g kg^{-1} for Al, Ca, Fe, K, and Mg; and 1 g kg^{-1} for S. The accuracy and analytical precision of the analytical method were verified against standard reference materials (OREAS 24P) and duplicate samples in each analytical set. The results were within the 95 % confidence limits of the recommended values for this certified material. Overall, analytical precision was ± 3 % for the major and trace elements analyzed.

Soil samples were submitted to multi-elemental analysis in ACME Anal. ISO 9002 Accredited Lab (Canada). Splits of 0.5 g were leached in hot (95 °C) aqua regia ($\text{HCl-HNO}_3\text{-H}_2\text{O}$) and concentrations were determined by inductively coupled plasma mass spectrometry (ICP-MS) for 36 elements: Ag, Al, As, Au, B, Ba, Bi, Ca, Cd, Co, Cr, Cu, Fe, Ga, Hg, K, La, Mg, Mn, Mo, Na, Ni, P, Pb, S, Sb, Sc, Se, Sr, Te, Th, Ti, Tl, V, W, and Zn (detection limits of Au <0.5 $\mu\text{g kg}^{-1}$; Hg

<0.01 mg kg⁻¹; Ag, Bi, Cd, Co, Cu, Mo, Ni, Pb, Sb, Sc, Th, Tl, W <0.1 mg kg⁻¹; Te <0.2 mg kg⁻¹; As, Se <0.5 mg kg⁻¹; Ba, Cr, Ga, La, Mn, Sr, Zn <1 mg kg⁻¹; V <2 mg kg⁻¹; B <0.02 g kg⁻¹; Na, P, Ti <0.01 g kg⁻¹; Al, Ca, Fe, K, Mg <0.1 g kg⁻¹; and S <0.5 g kg⁻¹). The accuracy and analytical precision were determined using analyses of reference materials (USGS standard) and duplicate samples in each analytical set. The results were within the 95 % confidence limits of the recommended values given for this certified material. The relative standard deviation (RSD) was between 5 and 10 %.

Mineralogical analysis

Minerals of the tailings, soil, and rock samples were determined by powder X-ray Diffraction (XRD) using a Phillips powder diffractometer, model PW3040/601, equipped with an automatic slit. A Cu-X-ray tube was operated at 40 kV and 30 mA. Data were collected from 2° to 70° 2θ with a step size of 1° and a counting interval of 0.6 s.

Selective chemical extraction

Two representative topsoil samples (A₁, A₂) characteristic from contaminated zones were used for the sequential extraction. The soil samples used in the selective chemical extraction (SCE) experiments were air-dried, disaggregated, homogenized, and sieved. A static approach to the leaching was adopted in this study. With the static approach, a sample will undergo sequentially a leaching process starting with the weakest to the strongest leach with subsequent analysis of each of the leachates by ICP-MS.

The fine-grained fraction of soil samples was submitted to sequential chemical extraction procedure in Activation Laboratories Ltd. (ACTLABS, see <http://www.actlabs.com>), accredited under ISO 9001 and 9002. Reagents were applied sequentially to the solid phase of selected samples, according to their chemical aggressiveness. The extractable fractions were obtained by extraction with different solutions: (a) fraction 1 (F₁)—sodium acetate (NaOAc, pH 5) for the extraction of exchangeable cations adsorbed by clay and those soluble in water or in slightly acidic conditions and co-precipitated by carbonates (the most labile bonded and therefore the most dangerous and bio-available for the

environment); (b) fraction 2 (F₂)—cold hydroxylamine for extracting amorphous Fe oxides and crystalline Mn oxides (metals bound to Fe and Mn oxides that can be released if conditions change from oxic to anoxic state); (c) fraction 3 (F₃)—hot hydroxylamine for the extraction of amorphous and crystalline Fe oxides and crystalline Mn oxides; (d) fraction 4 (F₄)—aqua regia, for leach sulfide species (metals which may be released under oxidizing conditions) and clay minerals; and (e) fraction 5 (F₅)—four-acid digestion (or total attack) where metals strongly associated with crystalline structures of minerals (such as the remaining silicates) will be decomposed (they are therefore unlikely to be released).

For Ag, As, Cd, Cu, Fe, Mn, W, and Zn, an internal check on the results was performed by comparing the sum of the five fractions from the sequential extraction procedure with the total amount obtained after hot mixed-acid attack of the same sample. These calculations can be used to validate the results and as inter-laboratory comparison. For all the extractions, the total of the trace elements in the different fractions did not exceed ±10 % of the bulk sample which is accepted as satisfactory. The relative extraction ratio was also calculated dividing the element concentration extracted by the individual leaching procedure by the concentration extracted by total attack (TA) as suggested by Son and Jung (2011).

Data analysis

Estimation of the regional and local geochemical baselines Environmental geochemical baselines are needed in order to assess the present state of the surface environment and provide guidelines and quality standards (Bini et al. 2011). Geochemical baseline is a term used to describe the natural background in areas of a heavy anthropogenic impact (Karim et al. 2015). Their definition was that a baseline encompasses the central 95 % of the observed concentrations. In this study, the geochemical baseline was determined using the Tuckey paradigm. First, the confidence range was determined, which excludes abnormal values—outliers. The geochemical baseline is considered to be the median of the data within the confidence range. The results were positively compared with those obtained with the Tidball and Ebens method (Levitan et al. 2014).

Principal component analysis Principal component analysis (PCA) is a method that aids in reducing the complexity of large-scale data sets and is currently broadly used in environmental impact studies by elucidate relations among variables by identifying common underlying processes (Abdi and Williams 2010). In the present study, a factorial analysis, PCA, was performed allowing reducing the size of the space of the variables. PCA main goal is to provide a small number of independent factors (principal components) which synthesize the associations between variables, being the referred factors (or PCs) orthogonal linear combinations of the variables. The first PC explains the major part of the total variance of the data set, and each successive PC explains a smaller part of the remaining variance. The different PCs are then related with common processes that affect the variables through expert knowledge of the problem in hand.

In order to characterize the studied area, PCA was applied. A matrix of 117 (samples) × 30 (chemical elements) of topsoil samples and a matrix of 113 (samples) × 30 (chemical elements) of subsurface soil samples were submitted to PCA. As stated previously, a regular grid (400 m×400 m; Fig. 1b) was used for soil sampling, and some of these samples (five topsoil and three subsurface soils) were taken over the tailing, for that reason and because tailing material is not a soil these samples were removed from the PCA study. According to the Kaiser criterion, a number of significant principal components with eigenvalue higher than 1 were selected (Fernandes-Caliani et al. 2009; Abdi and Williams 2010).

Spatial estimation Spatial estimation variography provides a description of the spatial pattern of a continuous attribute Z (or an indicator variable I_c), say a pollutant concentration of a chemical element or the anomalous concentration of a metal orebodies with economic interest. Given a data set for the variable Z at n locations x_i ($Z(x_i)$, $i=1, 2, \dots, n$), the sample variogram $\gamma_Z^*(h)$ (the asterisk in this text will indicate estimates) measures the average dissimilarity between data separated by a vector h (Garriguesa et al. 2008):

$$\gamma_Z^*(h) = \frac{1}{2N(h)} \sum_{i=1}^{N(h)} [Z(x_i) - Z(x_i + h)]^2$$

where $N(h)$ is the number of data pairs at a lag of h . For I_c , the variogram is

$$\gamma_{I_c}^*(h) = \frac{1}{2N(h)} \sum_{j=1}^{N(h)} [I_c(x_j) - I_c(x_j + h)]^2$$

The variogram can be calculated for different directions of h and allows to know how the variable $Z(x)$, or $I_c(x)$, varies in several directions of the space.

Ordinary kriging The main application of geostatistics to soil science has been the estimation and mapping of soil attributes in unsampled locations from nearby measured points in sampled areas. Kriging is a generic name for a family of spatial least squares predictors. For the prediction of the variable Z at a location x_0 , $\{Z(x_0)\}$, the estimator $Z^*(x_0)$ is defined as (Garriguesa et al. 2008)

$$Z^*(x_0) = \sum_{i=1}^n \lambda_i Z(x_i)$$

where the λ_i are weights found by solving the system of equations

$$\begin{cases} \sum_j^n \lambda_j \gamma(x_i, x_j) + \mu = \gamma(x_i, x), & i = 1, \dots, n \\ \sum_j^n \lambda_j = 1 \end{cases}$$

with $\gamma(h)$ being the theoretical model for the variogram of the variable Z (fitted to the sample variograms) and μ being a Lagrange multiplier.

The software used to create variograms, to model variograms and perform spatial estimation based on ordinary kriging (including map generation), was Surfer®v.11.

Pollution Load Index A quantitative approach of the multielement contamination was made based on the Pollution Load Index (PLI), by deriving the n th root of the n concentration factors ($CF_1 \times CF_2 \times CF_3 \times \dots \times CF_n$, where n is the number of metals). The concentration factor (CF) is defined as the ratio between each trace element in the soil sample and its background value. On account of the lognormal distribution of elements in geological materials, we assume the median (value at the 50th percentile of the background data) as soil geochemical baseline for each element, reflecting natural processes unaffected or diffusely affected by human activities (Cheng et al. 2014). According to Zhang et al. (2011), the PLI is divided in the following categories:

(a) $PLI=0$, background concentration; (b) $0 < PLI \leq 1$, unpolluted to moderately polluted; (c) $1 < PLI \leq 2$, moderately polluted; (d) $2 < PLI \leq 3$, moderately to highly polluted; (e) $3 < PLI \leq 4$ highly polluted; (f) $4 < PLI \leq 5$, very highly polluted; and (g) $PLI > 5$, extremely polluted.

Results and discussion

Statistical analysis, PCA analysis, and spatial geochemical interpretation

Table 1 resumes the summary statistics for the topsoil and subsurface soil sample data sets. In this table, also international and national literature reference soil values are presented. Casegas was chosen as regional geochemical background, once we had considered that this zone was out of the mining influence, located at NE upstream the mine location. The intention was the contents comparison between samples under mining influence and samples from a local background.

The comparative analysis reveals that Ag, As, Bi, Ca, Cd, Cu, P, and W maximum values in topsoil samples are higher than the concentrations of subsurface soil samples. On the other hand, elements such as Co, Fe, Mg, Mn, Mo, and Zn are higher on subsurface soil samples. According the results, it is possible to conclude that topsoil samples point to the anthropic contamination (geochemical signature of mineralization), while subsurface soils are related to the geogenic features (elements associated to geological formations). The comparison of topsoil and subsurface soil sample mean values with the local geochemical background values highlighted that As, Bi, Cd, and W elements are the most enriched (values ranging between 4 and 30 times). Arsenic and W mean concentrations obtained for both depths are significantly higher than the median values for Portuguese soils (MVPS) values (W: topsoil, 13.0 times, and subsurface soil, 4.1 times; As: topsoil, 9.3 times, and subsurface soil, 6.6 times; see Table 1). The mean As values exceeds also the enriched values for Portuguese soils (EVPS) (topsoil, 3.5 times; subsurface soil, As 2.5 times). In particular, the range of As contents in soils is larger than for the other elements in topsoil samples.

Table 1 shows that, in topsoil, the variables with highest skewness (values >3.0) are $Bi > Ca > As > Cr > W > P > Cu > Ag > Sb > Th > Sc > Cd$, while in

subsurface soils, the variables are $Ca > Sb > Cr > Bi > P > Ba > Cd > Sr > Mo$. The asymmetry observed in the data (Table 1) is due to the presence of outliers, which can endanger the spatial continuity of the variogram function and produce poor results when using parametric techniques like ordinary kriging. However, in this study, these difficulties are overcome as PCA produces new variables, the PCA components. PCA enabled the extraction of five PCs, for topsoil, explaining 69.09 % of the total variance. For subsurface soil, also five PCs were defined explaining 67.31 % of the total variance.

For topsoil samples, the first component (PC1) explains 13 (Ga, Cr, V, Sc, Ni, Fe, Al, Ba, Co, Th, La, K, Mg) of the 30 variables with 25.03 % of the total variance. Axis 2 (PC2) explains 12 variables (Cu, Cd, Ag, Zn, Sr, Ca, (As), Mn, P, Bi, (W) in opposition to Th; already explained in PC1) with a variance of 17.07 %. PC3 explains clearly five variables (As, Tl, Bi, Ti in opposition to Sr (also explained in PC2)) with 12.92 % of the total variance. The fourth component (PC4) explains two variables (K, Ti) already explained in PC1 and PC3, respectively, and has 8.00 % of the total variance. PC5 explains one variable (Se) with 6.07 % of the total variance.

For topsoil samples, the first component (PC1) explains 13 (Ga, Cr, V, Sc, Ni, Fe, Al, Ba, Co, Th, La, K, Mg) of the 30 variables with 25.03 % of the total variance. Axis 2 (PC2) explains 12 variables (Cu, Cd, Ag, Zn, Sr, Ca, (As), Mn, P, Bi, (W) in opposition to Th; already explained in PC1) with a variance of 17.07 %. PC3 explains clearly five variables (As, Tl, Bi, Ti in opposition to Sr (also explained in PC2)) with 12.92 % of the total variance. The fourth component (PC4) explains two variables (K, Ti) already explained in PC1 and PC3, respectively, and has 8.00 % of the total variance. PC5 explains one variable (Se) with 6.07 % of the total variance.

In the first factorial plan (PC1/PC2, Fig. 2a, representing 42.10 % of the global information of the data set), the selected variables could be separated into three groups. A first group (Group I: Al, Ba, Co, Cr, Fe, Ga, K, La, Mg, Ni, Sc, V) with positive loadings in PC1 reveals an association of elements strongly correlated between them (Spearman correlation coefficient higher than 0.70: Sc-V ($r=0.88$), Cr-V ($r=0.80$), Cr-Ga ($r=0.80$), Al-Ga ($r=0.77$), Mg-Ni ($r=0.77$), Fe-Ga ($r=0.75$), Co-Ni ($r=0.74$), Cr-Fe ($r=0.74$), Ga-V ($r=0.74$), Al-Cr ($r=0.73$); $p < 0.01$) with small variability and represents an association of lithological elements

Table 1 Range and median value concentrations of topsoil and subsurface soil samples in Panasqueira mine and surrounding environment compared with data from international literature

Var.	Unit	Soil ₀ (n=122)				Soil ₁₅ (n=116)				Geochemical baselines			Data from literature
		Min–Max	MD	Mean	Sk	Min–Max	MD	Mean	Sk	Soil ₀	Soil ₁₅	Bk	
Ag	mg kg ⁻¹	0.05–1.7	0.1	0.2	4.72	0.1–0.6	0.1	0.1	1.98	0.1	0.1	0.05	0.07 ^a
Al	g kg ⁻¹	6.3–30	17	17	0.37	8.5–37	20	20	0.27	20	20	18	80 ^a
As	mg kg ⁻¹	17–1503	65	102	6.98	8–350	52	73	2.05	63	49	22	11 ^b
Ba	mg kg ⁻¹	10–155	32	36	2.90	9–145	28	31	3.72	31	27	41	210 ^c
Bi	mg kg ⁻¹	0.3–65	0.9	1.9	9.21	0.2–15	0.6	1.1	5.51	0.8	0.6	0.3	0.3 ^a
Ca	g kg ⁻¹	0.1–13	0.5	0.8	7.42	0.1–8.4	0.1	0.3	76.5	0.5	0.1	0.3	140 ^a
Cd	mg kg ⁻¹	0.1–3.0	0.2	0.3	3.77	0.1–1.5	0.1	0.2	3.65	0.2	0.1	0.01	0.3 ^a
Co	mg kg ⁻¹	1–36	6	7	2.63	1–63	7	8	4.20	6	7	7	8 ^b
Cr	mg kg ⁻¹	10–166	26	28	6.85	10–155	30	32	5.73	25	30	27	21 ^b
Cu	mg kg ⁻¹	10–292	35	42	4.80	12–146	33	38	2.86	34	31	28	16 ^b
Fe	g kg ⁻¹	17–55	31	30	0.80	19–64	33	34	1.17	30	30	33	27.4 ^b
Ga	mg kg ⁻¹	3–10	5	5	0.81	3–9	6	6	0.19	5	6	5	n.a.
K	g kg ⁻¹	0.4–4.1	1	1.2	1.96	0.3–3.8	0.8	0.5	1.56	0.9	0.8	1.3	140 ^a
La	mg kg ⁻¹	8–52	18	18	2.06	12–48	20	21	1.75	18	20	18	35 ^a
Mg	g kg ⁻¹	0.4–6.6	2.6	2.9	0.41	0.2–8.5	2.8	3	0.62	2.6	2.7	3.6	9 ^a
Mn	mg kg ⁻¹	30–653	141	177	1.69	21–840	113	156	2.42	124	99	175	394 ^b
Mo	mg kg ⁻¹	0.2–1.0	0.4	0.5	0.92	0.2–2.2	0.5	0.5	3.18	0.4	0.5	0.5	0.5 ^b
Ni	mg kg ⁻¹	6–74	18	20	2.29	5–69	22	22	1.29	18	21	22	16 ^b
P	g kg ⁻¹	0.26–3.2	0.39	0.49	5.27	0.23–2.5	0.38	0.45	4.45	0.3	0.3	0.5	0.75 ^a
Pb	mg kg ⁻¹	9–97	27	30	1.79	7–113	24	28	2.11	26	23	23	21 ^b
Sb	mg kg ⁻¹	0.05–3.5	0.40	0.46	4.44	0.1–5.6	0.3	0.3	6.50	0.3	0.3	0.7	1.0 ^c
Sc	mg kg ⁻¹	0.7–7.2	1.3	1.5	3.84	0.9–7.1	1.8	2.0	2.41	1.3	1.8	1.7	12 ^a
Se	mg kg ⁻¹	0.3–1.7	0.6	0.6	0.86	0.3–1.8	0.3	0.5	1.20	0.6	0.3	0.4	0.3 ^a
Sr	mg kg ⁻¹	1–25	6	8	1.56	1–27	3	4	3.57	6	3	6	240 ^a
Th	mg kg ⁻¹	0.7–22	4.8	4.9	3.97	1.6–21	6.3	6.3	1.90	4.8	6.2	3.8	1.0 ^d
Ti	mg kg ⁻¹	10	60	120	1.92	1	50	120	1.57	100	100	30	4000 ^a
Tl	mg kg ⁻¹	0.1–1.3	0.2	0.2	2.17	0.1–1.1	0.2	2.3	1.81	0.2	0.2	0.05	1 ^c
V	mg kg ⁻¹	10–71	25	26	1.51	14–69	28	30	1.17	25	28	23	27 ^b
W	mg kg ⁻¹	0.2–200	6	13	5.40	0.1–29	2.7	4.1	2.51	4.4	2.5	0.4	1.0 ^b
Zn	mg kg ⁻¹	22–199	70	77	1.38	16–192	70	75	1.08	68	68	58	55 ^b

MD median values, Sk skewness, n.a. not available

^a Mean world soils (Deschamps et al. 2002; Reimann and Caritat 1998)

^b Median values for Portuguese soils (Ferreira 2004)

^c Ontario reference values (Ministry of the Environment 2011)

^d Normal ranges in soils (Fiedler and Rösler 1993; Mench 1993; Radojevic and Bashkin 1999)

driven by local geology. In this group, it is possible to separate two sub-sets: one with positive loadings in PC1 and negative loadings in PC2 (Al, Cr, Fe, Ga, Tl, Ni, Sc, V variables) and another with positive loadings in PC1 and PC2 (Ba, K, Mg, Ni variables). These two sub-sets

allow the separation between the argillaceous shales and the spotted argillaceous shales (Ba, K, Mg, Ni enrichment; see Table 2).

The group related to PC2 (group III: Ag, As, Bi, Ca, Cu, Cd, Mn, P, Sr, W) reveals elements strongly

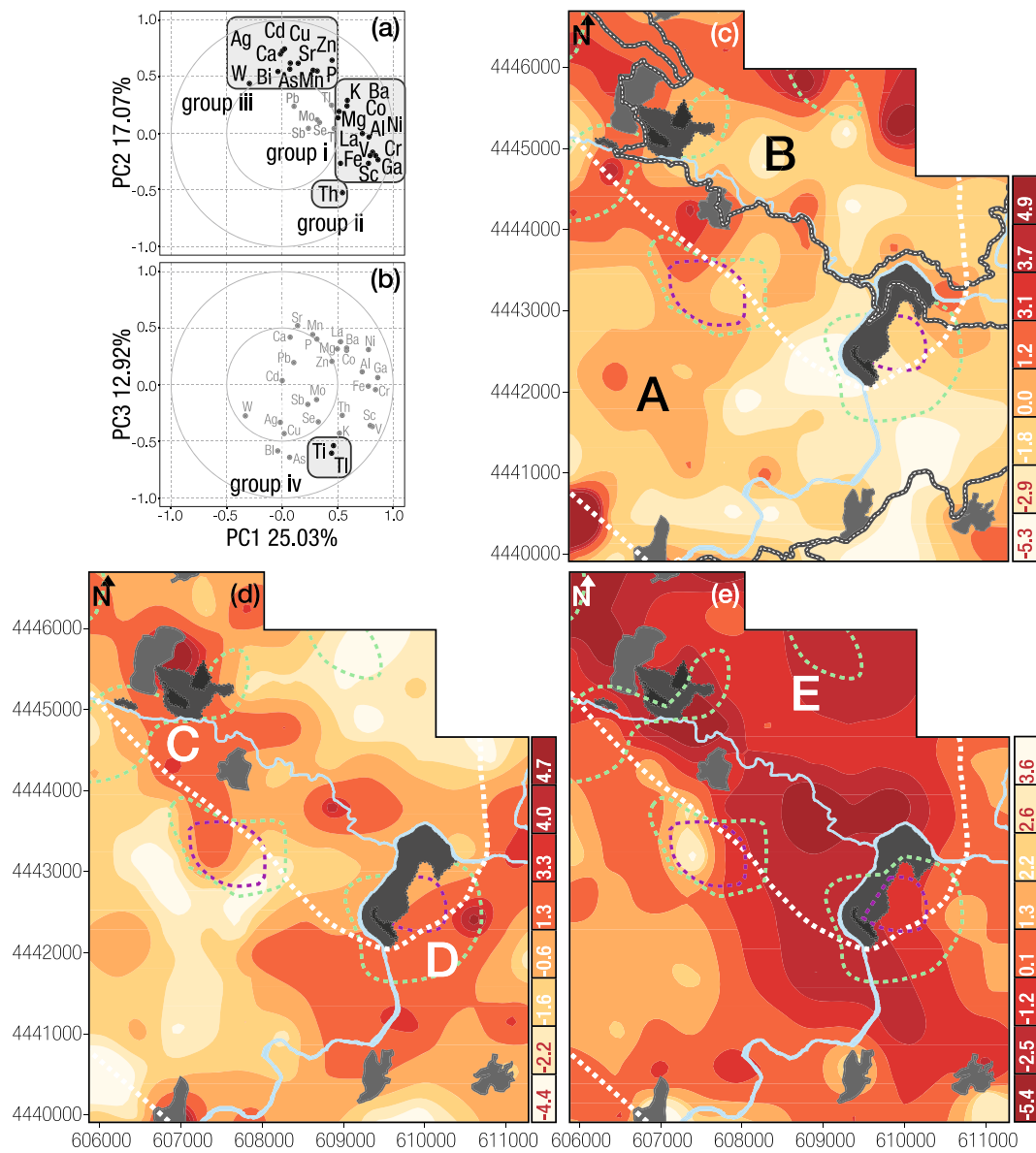


Fig. 2 Variable projection of topsoil samples on **a** PC1/PC2 and **b** PC1/PC3 factorial plans and score value spatial distribution of the selected principal components (PCs) on the simplified map of the studied area: **c** PC1 (Ga, Cr, V, Sc, Ni, Fe, Al, Ba, Co, Th, La, K, Mg; positive scores), **d** PC2 (Cu, Cd, Ag, Zn, Sr, Ca, As, Mn, P,

Bi; positive scores), and **e** PC3 (Ti, Tl; negative scores). The *white dashed lines* represent the geological contacts shown in Fig. 1; the *green dashed lines* represent the highly anomalous areas; the *purple dashed lines* represent the very highly anomalous areas, according to Cavey and Gunning (2006)

correlated between them and with strong positive skewness ($Sk > 3.0$, Table 1). Spearman correlation coefficient showed $r \geq 0.7$ ($p < 0.01$) between As-Bi ($r = 0.87$), Bi-Cu ($r = 0.78$), As-Cu ($r = 0.77$), Bi-W ($r = 0.77$), Cd-Cu ($r = 0.74$), and Ag-Cu ($r = 0.73$).

The second factorial plan (PC1/PC3, representing 37.95 % of total variance) is dominated by the association of Tl and Ti variables (group IV).

One of the main goals of this study is to assess the extent of the soil pollution due to the present and past mining activities and erosion of the tailing materials. To determine the spatial geochemical structure of the variables defined by the PCA, experimental variograms were constructed and modeled. All variograms were modeled with exponential functions. Table 3 shows the parameters of

Table 2 Concentration values of rock samples

Var	Unit	DL	Sch ₁	Sch ₂	Sch _{sp}	QZ	QZ _{sp}
Ag	mg kg ⁻¹	0.1	0.1	0.2	0.2	<0.1	0.1
Al	g kg ⁻¹	0.1	106	70	75	48	46
As	mg kg ⁻¹	1	14	87	405	37	21
Ba	mg kg ⁻¹	1	580	491	529	365	264
Bi	mg kg ⁻¹	0.1	0.5	0.5	0.6	0.3	0.3
Ca	g kg ⁻¹	0.1	0.3	0.3	0.6	0.8	1
Cd	mg kg ⁻¹	0.1	<0.1	0.2	0.3	<0.1	<0.1
Co	mg kg ⁻¹	0.2	13	5.2	9.3	5	12
Cr	mg kg ⁻¹	1	124	98	112	75	84
Cu	mg kg ⁻¹	0.1	47	36	54	14	18
Fe	g kg ⁻¹	0.1	58	43	53	28	33
K	g kg ⁻¹	0.1	30	26	29	16	12
La	mg kg ⁻¹	0.1	15	17	14	23	21
Mg	g kg ⁻¹	0.1	8.4	15	16	8.9	9.7
Mn	mg kg ⁻¹	1	219	432	376	184	287
Mo	mg kg ⁻¹	0.1	0.2	<0.1	<0.1	0.2	0.1
Na	g kg ⁻¹	0.01	0.8	12	7.8	13	15
Ni	mg kg ⁻¹	0.1	46	24	57	26	34
P	g kg ⁻¹	0.01	0.4	0.5	1	0.4	0.6
Pb	mg kg ⁻¹	0.1	12	3	11	3.7	6.3
Sb	mg kg ⁻¹	0.1	1.2	0.6	<0.1	0.2	0.1
Sc	mg kg ⁻¹	1	18	12	13	8	8
Se	mg kg ⁻¹	1	<1	1	<1	1	<1
Sr	mg kg ⁻¹	1	25	26	32	34	41
Th	mg kg ⁻¹	0.1	6.9	7.4	6.4	7.5	7.2
Ti	g kg ⁻¹	0.01	4.4	6	6.2	4.3	4.1
Tl	mg kg ⁻¹	0.5	0.7	1.2	0.8	0.6	<0.5
V	mg kg ⁻¹	1	184	149	179	89	90
W	mg kg ⁻¹	0.1	1.3	4.6	3.4	3.2	3
Zn	mg kg ⁻¹	1	136	427	252	78	89

DL detection limit, Sch₁ argillaceous shales, Sch₂ argillaceous shales, Sch_{sp} argillaceous spotted shales, QZ quartzites, QZ_{sp} spotted quartzites

model function fitted to the experimental variograms of the three PCs retained.

Figure 2c–e shows the spatial distribution of the selected factors allowing the identification of the geochemical/geological processes within the study area in what concerns to topsoil samples.

The high positive score values on PC1 topsoil map (Fig. 2c) indicates geochemical anomalies correlated to the local geology. Geologically, the studied area is divided in two general geological units (Fig. 1b): the western area (A) contains argillaceous shales, schists, and quartzites. Mineralogically, the shales are composed of quartz, chlorite ((Mg,Fe)₃(Si,Al)₄O₁₀(OH)₂. (Mg,Fe)₃(OH)₆), biotite ((Mg,Fe)₃[AlSi₃O₁₀(OH,F)₂]),

and sericite, locally with the presence of Fe oxides and hydroxides.

The eastern area (B), due to the influence of the contact metamorphism with the granite intrusion, is underlain dominantly by argillaceous spotted shales (chlorite ± biotite ± moscovite/sericite and, according to some authors, cordierite (Mg₂Al₄Si₅O₁₈), schists, and quartzites (Polya 1989). It is also important to mention that the Beira schist formation was subjected to lower greenschist grade regional metamorphism during the early compressive stages of the Hercynian Orogeny. Polya (1989) established the following paragenetic association for regional metamorphism of pelitic series: quartz-albite-chlorite-muscovite-paragonite. According

Table 3 Parameters of model function fitted to the experimental variograms of the three PCs retained for topsoil and subsurface soil and the Pollution Load Index (PLI)

ID	Model	Main direction	C ₀	C ₁	Length	Anisotropy ratio	
Soil ₀ PCA	PC1	exponential	30	0.0	9.0	1100	1.98
	PC2	exponential	30	0.0	5.5	1100	2.77
	PC3	exponential	0	1.3	6.0	1000	1.99
Soil ₁₅ PCA	PC1	exponential	65	4.1	3.1	1000	2.19
	PC2	exponential	65	2.3	4.1	900	2.01
	PC3	exponential	45	0.2	2.3	900	2.72
PLI	Soil ₀	exponential	90	2.1	30.0	900	1.41
	Soil ₁₅	exponential	90	2.6	4.3	1000	2.48

PCA principal component analysis

to this author, the metasediments present high Al₂O₃ concentrations and low CaO concentrations as confirmed in Table 2. The metasediments with a coarser granulometry show higher SiO₂ and TiO₂ concentrations and smaller concentrations of Fe₂O₃, K₂O and Nb. According to Table 2, the spotted schists are enriched in As, Mg, and Mn when compared with the argillaceous schists sampled in Casegas (background area). Few mafic rocks (dolerites) were observed, particularly near S. Jorge da Beira (NW-SE subvertical). The rock is fine grained and micro-porphyratic and chiefly consists of labradorite ((Ca,Na)(Al,Si)₄O₈), and amphibolitized pyroxene. Also, quartz veins, parallel to the schistosity, are related to the low grade of metamorphism (Thadeu 1951).

The spatial distribution of topsoil PC2 (positive scores; Fig. 2d) reveals a separation of soil samples influenced by the proximity to pollution sources, and also from past mining activities during the WWI and WWII periods (locally named as “Kilo”). This group appears to be controlled by the geochemical signature of the sulfide mineralization, once all the elements presented in this factor are representative of the paragenesis associated to the different phases. These elements still maintain a close relationship in the secondary environment. Silver minerals with a high Ag content such as matildite (AgBiS₂) may be responsible for a great part of the silver present in samples. Argentiferous stannite (Cu₂(Fe,Zn)SnS₄) will also contribute to the total amount of silver present in the chalcopryrite concentrate, as stannite is a common minor constituent. Other rare minerals such as canfieldite (Ag₈SnS₆) and pavonite ((Ag,Cu)(Bi,Pb)₃S₅) play also a subordinate role as contributors of silver. All these minerals mainly occur in chalcopryrite and they are extracted with the chalcopryrite concentrate. Minor silver, however, is lost in the

sulfide tailings (Wimmers 1983). This can be explained by the presence of some of the matildite in arsenopyrite, which goes into the tailings. According to Ferreira da Silva et al. (2013), these associations represent the strong influence of the Barroca (C; Fig. 2d) and Rio tailings (D; Fig. 2d). The mud dams (in Rio and Barroca Grande) contain high levels of As, Cd, Cu, and Zn. According to these authors, the Rio tailing samples contained abundant amounts of scorodite (FeAsO₄•2H₂O), sphalerite (ZnS), wolframite (FeWO₄), quartz, natrojarosite (NaFe₃(SO₄)₂(OH)₆), vermiculite ((Mg,Fe,Al)₃(Al,Si)₄O₁₀(OH)₂•4H₂O), montmorillonite ((Mg,Ca)O•Al₂O₃Si₅O₁₀•nH₂O), illite, some silicates like kaolinite (Al₂Si₂O₅(OH)₄), and sulfate minerals, while in Rio tailings dam, melanterite (Fe(SO₄)•7(H₂O)) and minor amounts of rozenite (Fe(SO₄)•4(H₂O)) and szomolnokite (Fe(SO₄)•(H₂O)) were observed by XRD identification. The Rio dam consists predominantly of quartz, mica, feldspar, illite-vermiculite, arsenopyrite, marcasite, pyrite, pyrrhotite, and chalcopryrite. Other minerals, like scorodite and natrojarosite, are also present. The XRD analysis of the active dam sample of Barroca Grande revealed the presence of scorodite, arsenopyrite, quartz, sphalerite, hematite (Fe₂O₃), and muscovite (KA₂(AlSi₃O₁₀)(F,OH)₂), while the sample from the old dam of Barroca Grande contained quartz, pyrite, chalcopryrite, wolframite (ferberite), and scorodite (Ávila et al. 2008b). Sample collected in the tailing materials of Barroca Grande consists predominantly of arsenopyrite, wolframite (ferberite), quartz, and muscovite. The presence of P, Sr, and Ca variables in this association could represent the influence of the late carbonate phase of the paragenesis. In this phase, is possible to identify calcite (CaCO₃) and dolomite (MgCO₃). Other rare minerals are found such as

thadeuite ((Mg(Ca,Mn)(Mg,Fe,Mn)₃(PO₄)₂(OH,F)₂) and panasqueirite ((Ca,Mg)PO₄(OH,F)). Thadeu (1951) refers also to the presence of carbonates in metasediments related to the hydrothermal weathering and Bloot and de Wolf (1953) relates the presence of carbonates to diagenesis process. Sousa (1985) refers also to the occurrence of phosphatic levels, in the conglomeratic sequences.

The association of group III is essentially anthropogenic and is related to the minerals belonging to the primary paragenesis, such as arsenopyrite (FeAsS), bismuthinite (Bi₂S₃), and rutile (TiO₂), rejected during the tungsten separation process and cumulated in the tailing and mud dam. The interaction water-minerals at the waste dump surface leads to the generation of acid mine drainage with high contents of metals and sulphate, related to the sulfides alteration. The alteration degree of these sulfides is recorded in the geochemical evolution of the primary paragenesis and leads to the emergence of a new mineralogy with neof ormation minerals, such as scorodite, melanterite, szomolnokite, and rozenite. These secondary minerals play an important role in the natural retention of oxyanions and divalent cations like Cu, Zn, and Pb, for example, due to the element capture by sorption and precipitation, and the precipitation and dissolution of such secondary minerals are processes strongly influenced by seasonal wetting and drying cycles. Climate can be an important instability factor, and in this region, it is aggressively very hot and dry during summer and very cold, rainy, and windy in the winter. Due to these phenomena, soils appear to be a good receptor of some of the metals present in the primary and also the secondary mineralogy.

For subsurface soils, five PCs were extracted which explain 56.66 % of the total variance. The first component (PC1) explains 16 variables (Ni, Fe, Ga, Zn, Sc, V, Al, Cr, Cu, Mn, Co, K, P, Ba, Mo, Ti) of the 30 variables with 27.93 % of the total variance. The second component (PC2) explains six variables (Ca, Cd, Sr, P in opposition to Th and V) with 14.75 % variance. The third component (PC3) explains two variables (W, As, and Tl, already explained also by PC1) in opposition to Ba and Sr (explained in PC1), with 10.56 % variance. PC4 explains one variable (Mo) having 7.76 % variance and PC5 explains the two variables (Mg, Al) with 6.30 % variance.

The subsurface soil samples projection of the 30 variables studied on the two factorial planes are showed in Fig. 3a, b. Eight groups of variables can be identified.

The subsurface soil Axis 1 is formed by group I—Al, Co, Cr, Cu, Fe, Ga, Mn, Ni, Sc, V, Zn variables (Fig. 3a)—representing a mixture between the geogenic factor (Al, Cr, Fe, Ga, Ni, Sc, Tl, V; association separated by negative scores of axis 2) and the influence of the geology and paragenesis (As, Co, Cu, Zn; separated by positive scores of axis 2). Axis 2 represents the association of group III (Ca, Cd, P, Sr) and group II (Th) (Fig. 3a). Axis 3 is formed by group IV (As, Tl, W negative scores). Four other groups were formed: group V (K, Ti) and group VI (Mo) on the axis 4 and group VII (Sb) and group VIII (Mg) in axis 5. Spearman correlation coefficient showed strong correlations ($r \geq 0.7$, $p < 0.01$) between Cr-Ga ($r=0.87$), K-Ti ($r=0.85$), Ti-Tl ($r=0.83$), As-Bi ($r=0.83$), Sc-V ($r=0.82$), Cr-V ($r=0.82$), Ga-V ($r=0.81$), Co-Mn ($r=0.81$), K-Tl ($r=0.79$), Al-Ga ($r=0.77$), Mg-Ni ($r=0.77$), Ti-V ($r=0.76$), Mg-Zn ($r=0.75$), Co-Ni ($r=0.73$), Sc-Ti ($r=0.72$), Fe-Ga ($r=0.72$), and Ni-Zn ($r=0.71$).

Figure 3c–e shows the spatial distribution of the selected factors of subsurface soils allowing the identification of the geochemical/geological processes within the study area.

The estimated map of the subsurface soil samples PC1 spatial distribution can be observed in Fig. 3c. High positive values indicate that geochemical anomalies lie within the local geology. PC1 mapping allow a better separation between the area related to the argillaceous spotted schists (B) and the argillaceous schists. In this case, As variable represents a mixture between the geogenic and the anthropogenic factor (due to the enrichment of the argillaceous spotted schists and also the influence of the Barroca and Rio tailings and mud impoundments; see Table 2). PC2 spatial distribution identifies clearly the areas near the tailings and also the presence of the dolerite rocks. As observed in topsoil samples the association between As and Tl is also clear in subsurface soil samples and identifies the area with the argillaceous spotted schists.

Pollution Load Index and environmental considerations

As noted on topsoil sample PCA results, Ag, As, Bi, Cd, Cu, W, and Zn are the most important variables to estimate the PLI on each sample (Table 4). Figure 4 displays the spatial distribution of the Pollution Load Index estimated.

In topsoil samples, the highest mean pollution load index ($PLI_{\text{mean}}=14$, classified as extremely polluted)

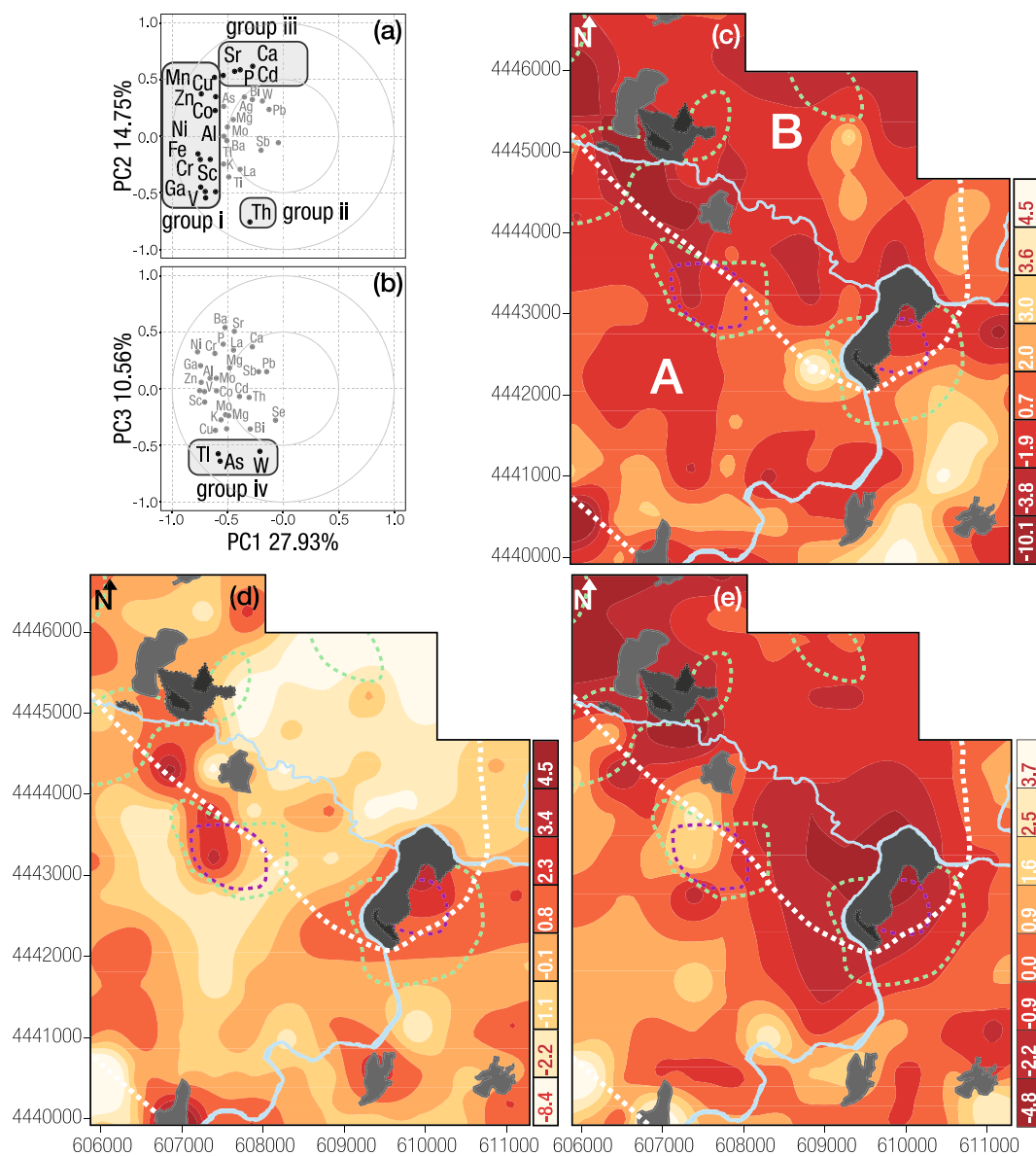


Fig. 3 Variables projection of subsurface soil samples on **a** PC1/PC2 and **b** PC1/PC3 factorial plans and score value spatial distribution of the selected principal components (PCs) on the simplified map of the studied area: **c** PC1 projection (Ni, Fe, Ga, Zn, Sc, V, Al, Cr, Cu, Mn, Co, K, P, Ba, Mo, Ti; negative scores), **d** PC2 projection (Ca, Cd, Sr, P; positive scores), and **e** PC3 projection

(W and also As, Ti; negative scores). The *white dashed lines* represent the geological contacts shown in Fig. 1; the *green dashed lines* represent the highly anomalous areas; the *purple dashed lines* represent the very highly anomalous areas according to Cavey and Gunning (2006)

was registered in Rio mostly due to the high concentrations of W and Cd in this area that exceed the background value, respectively, as much as 245 and 107 times. Also, the highest concentrations of Bi, Ag, and As were found in Rio soil samples. Only Zn presents in Barroca Grande soils slightly higher concentrations than in Rio samples. The concentration factor (CF) values,

determined in Rio, were very high mainly due to W (up to 571), Cd (up to 300), Bi (up to 215), Ag (up to 34), and As (up to 14). According to these results, the Rio area contains very high levels of potentially toxic elements (PTEs), even if the total concentrations are conditioned by the sample locations; for example, As values range from 53 to 3640 mg kg⁻¹, with a mean value of

Table 4 Mean and range of concentration factors (CF_x for the selected elements) and related Pollution Load Index (PLI) of the global data (soils and tailing), Barroca Grande and Rio areas, and the local geochemical baseline values (Casegas)

		Global area (n=122/116)			Barroca Grande (n=14/15)			Rio (n=10/10)			Casegas (n=47)		
		Mean	Min	Max	Mean	Min	Max	Mean	Min	Max	Mean	Min	Max
Soil ₀	CF _{Ag}	3	1.0	34	5	1.0	20	10	2	34	2	1.0	8
	CF _{As}	5	0.8	68	7	2	15	14	2	68	1.2	0.4	5
	CF _{Bi}	6	1.0	215	6	2	12	34	2	215	1.3	0.7	9
	CF _{Cd}	30	5	300	50	5	150	72	10	300	9	1.0	30
	CF _{Cu}	1	0.4	10	2	0.7	8	3	1.0	10	1.1	0.6	6
	CF _W	38	0.6	571	31	2	89	179	5	571	3	0.1	26
	CF _{Zn}	1.3	0.4	3	2	0.7	3	1.4	0.9	3	1.1	0.3	2
	PLI	5	1.0	57	7	2	15	14	2	57	1.6	0.5	6
Soil ₁₅	CF _{Ag}	3	1.0	12	3	1.0	10	3	1.0	10	n.a.	n.a.	n.a.
	CF _{As}	3	0.4	16	6	2	13	5	2	12	n.a.	n.a.	n.a.
	CF _{Bi}	4	0.7	51	9	1.7	51	4	1.3	14	n.a.	n.a.	n.a.
	CF _{Cd}	17	5	150	34	5	150	29	5	80	n.a.	n.a.	n.a.
	CF _{Cu}	1.3	0.4	5	2	0.8	4	2	0.8	5	n.a.	n.a.	n.a.
	CF _W	12	0.1	84	17	1.4	41	26	1.7	84	n.a.	n.a.	n.a.
	CF _{Zn}	1.3	0.3	3	2	0.7	3	1.3	0.3	3	n.a.	n.a.	n.a.
	PLI	3	0.7	15	6	2	12	5	1.4	15	n.a.	n.a.	n.a.

n number of topsoil samples/number of subsurface soil samples, n.a. not applicable

710 mg kg⁻¹ and a background value of 22 mg kg⁻¹. The total abundance of Ag, Bi, Cd, and W mean concentrations are 32, 55, 107, and 245 times, respectively,

higher than the background value defined in Casegas area. Although the CF values, determined for Cu (10) and for Zn (3), are significantly lower than the CFs

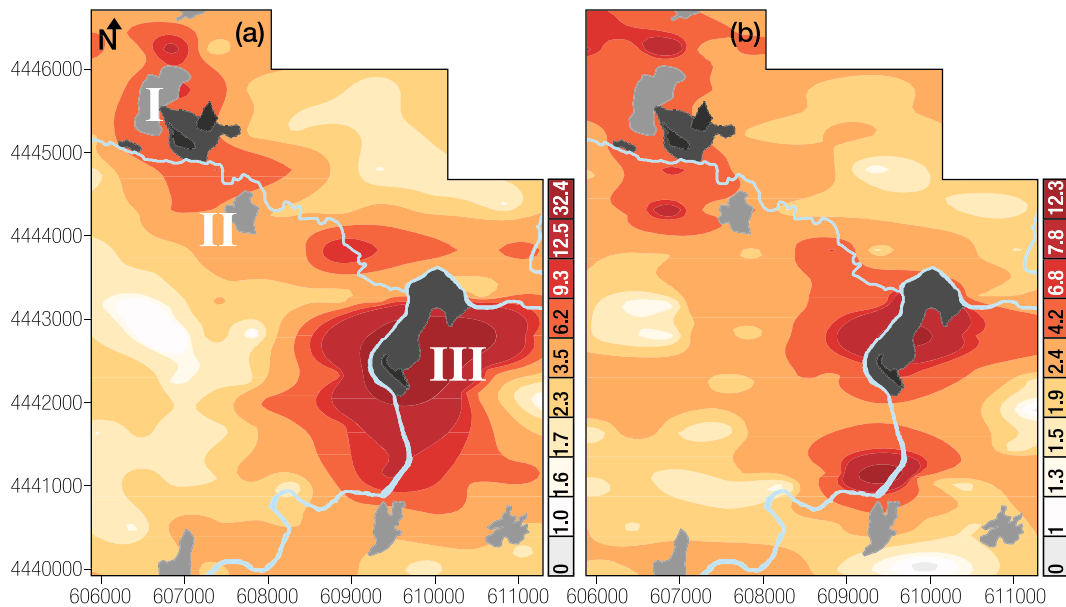


Fig. 4 Pollution Load Index (PLI) mapping for topsoil (a) and subsurface soil (b) samples. Values were estimated on the basis of the concentration factors of Ag, As, Bi, Cd, Cu, W, and Zn (I, Barroca Grande; II, S. Francisco de Assis; III, Rio)

determined for the others elements, both Cu and Zn present results above 1 (Table 4).

In Barroca Grande area, the PLI results for topsoil samples range between 2 and 15, with a mean value of 7 (extremely polluted). The CF is also high, especially for Cd (up to 150), W (up to 89), Ag (up to 20), and As (up to 15). According to these results, Barroca Grande contains very high concentrations of Cd, W, Ag, and As, being higher than the background levels, respectively, 47, 30, 5, and 7 times.

Subsurface soils also present higher maximum PLI values in Rio area (up to 15), mostly due to the high concentrations of W, which are 42 times higher than the background guide value. Also, Cd, Bi, and As present high soil concentrations. Barroca Grande subsurface soil samples present a higher mean PLI result (7), and also the CF of Cd (up to 150), Bi (up to 51), and As (up to 13) present the higher values. Cadmium, W, Bi, and As have the highest concentrations in this area, being respectively 32, 17, 9, and 6 times higher than the background values.

The PLI values are indicative of serious soil pollution. The results clearly point out that soils collected near the waste tailings presents higher contamination indices than the soil samples collected in the mine surroundings. In both areas (Fig. 4), the mine wastes are a mixture of weakly to strongly sulfidic rock and non-mineralized host rock materials.

According to Ávila et al. (2008b), the materials collected in the active and old dam and tailing of Barroca Grande and in the Rio tailing and mud impoundment revealed very high concentrations of Ag, As, Cd, Cu, V, Mn, W, and Zn. The highest PLI values identified near Barroca Grande (I), São Francisco de Assis (II), and Rio (III) confirms that the mechanical and chemical dispersion continuously occur from Barroca Grande and Rio tailings and mud impoundments. Most of the samples ($\geq 70\%$ total samples) collected in Barroca Grande (I), São Francisco de Assis (II), and Rio (III) locations have mean PLI values >7.0 , clearly showing a very high degree of contamination.

Chemical forms of heavy metals in soils directly influence their bioavailability and toxicity (Violante et al. 2010). Trace metals can be transported in the secondary geological environment by different chemical mechanisms (Akai and Anawar 2013): (a) in solution or adsorbed on solids, being readily available in these conditions; (b) in organic compounds or metallic hydroxides, for which chemical changes are required before they are released; and (c) in the crystal structure of

some minerals, where they are generally unavailable for the ecosystems. Two soil samples (A1 and A2; selected according their PLI spatial distribution) were submitted to sequential chemical extraction in order to estimate the distribution of Ag, As, Cd, Cu, Fe, Mn, W, and Zn among the geochemical bearing phases, which accounts for the relative proportions of each trace metal transported by the mechanical and chemical agents. Figure 5 shows the geochemical partitioning of some selected elements in those fractions of each sample.

According to the results, As is linked to sulfides since a considerable proportion is extracted by aqua regia (F_4 ; 66.7 to 68.4 %) which reflects the presence of arsenopyrite in the analyzed samples. The amorphous and crystalline Fe and Mn oxyhydroxides (F_3) are also important bearing phases of this element. The percentage of easily mobilized phases is very low (0.04 to 0.05 %); however, the related As concentration values (0.4–0.7 mg kg⁻¹) could be considered very high. Silver, Cd, Cu, and Mn show similar SCE patterns suggesting that these elements are linked to amorphous Fe/Mn oxyhydroxides and also to sulfide or clay minerals (part of these elements was extracted with aqua regia). Cadmium was also greatly extracted with sodium acetate (10.3 to 13.9 % of extraction; 1.9 to 4 mg kg⁻¹ for Cd) indicating that soluble/exchangeable/carbonate fraction is the preferential sink for Cd. Iron is mostly extracted by aqua regia (step 4; percentage of extraction ranging from 39.2 to 69.3 %), suggesting also the presence of sulfides. However, considerable proportion of this metal (up to 50 % in sample A1) appears to be also associated to the remaining silicates. It must be pointed out that the percentage of extraction associated to amorphous and crystalline Fe and Mn oxyhydroxides ranges between 8.3 and 9.4 %. The highest percentage of W extraction, related to the last two steps of extraction, shows that W is highly resistant to both chemical and physical weathering and can be transported long distances from the source areas. The mobility of W is intermediate to low in neutral pH water (Bednar et al. 2009). The principal ore mineral, wolframite, is similar to cassiterite in resistance to chemical weathering but is somewhat less resistant than cassiterite to physical weathering. Tungsten minerals are brittle and readily break down into fine particles that disperse in fine-grained sediment. Zinc is mainly associated with amorphous Fe oxides and crystalline Mn oxides and clays. The results also show also that a significant percentage of this element could be released under oxidizing conditions.

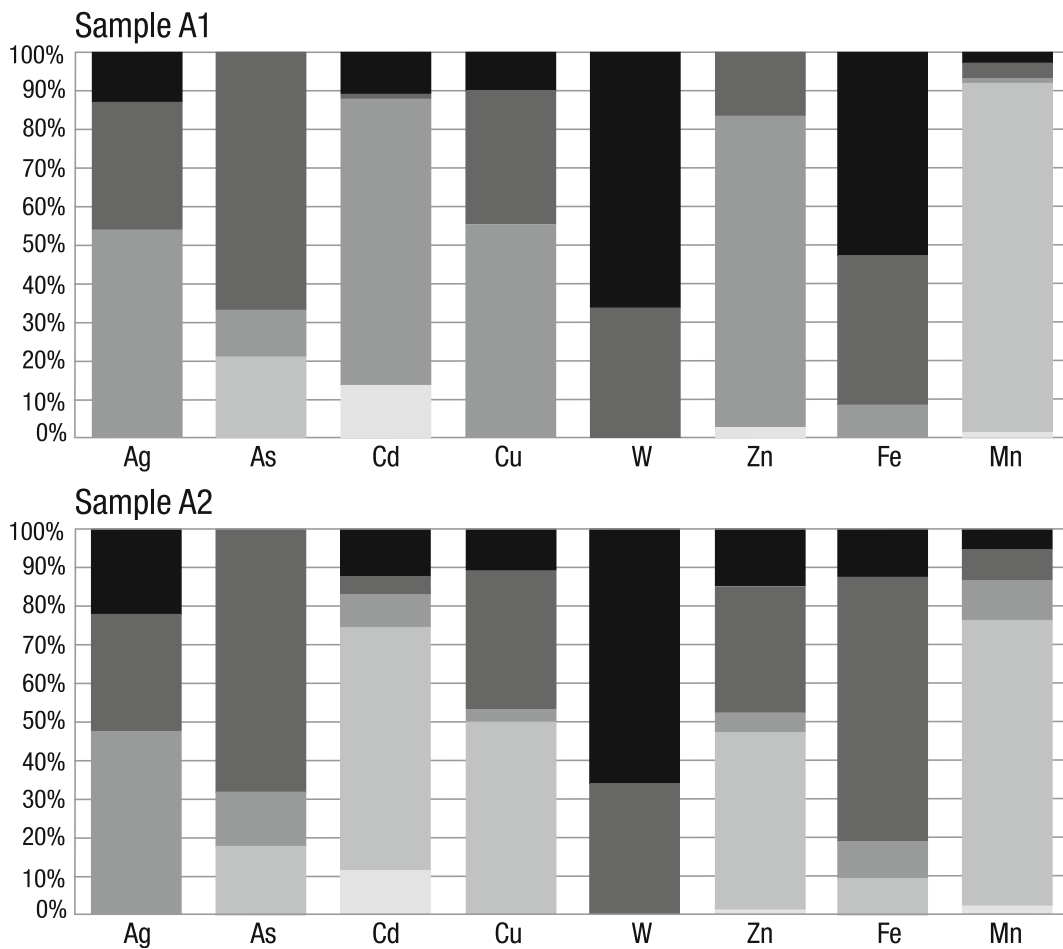


Fig. 5 Relative extraction ratio values of Ag, As, Cd, Cu, Fe, Mn, W, and Zn in each step of the sequential extraction procedure (F1, easily soluble fraction; F2, amorphous Fe oxides and crystalline Mn oxides; F3, amorphous/crystalline Fe and crystalline Mn oxides; F4, metals released under oxidizing conditions and clay minerals; and F5, residual fraction)

The results of the environmental risk assessment according to risk assessment code (RAC) show that most of the elements are classified in the low risk category except Cd that posed low to medium risk (results of percentage of extraction ranges from 10 to 13 % of extraction associated to F₁). This soluble/exchange fraction (F₁) is a loosely bound phase and liable to change with environmental conditions such as pH changes (Xie et al. 2013). However, metals associated with F₂ are thermodynamically unstable and must be considered as direct effect phases. Considering both F₁ and F₂ results, Ag, Cd, Cu, and Zn are classified as *very high risk* in the two analyzed samples, while As is classified as *medium risk*. Tungsten presents *no risk* which is consistent with their strong resistance to chemical weathering.

Result comparison with similar studies

Soil heavy metal pollution has become a severe problem in many parts of the world. Although heavy metals may occur naturally in soils, additional contributions come from anthropogenic activities, one of them being the mining industry. Numerous studies have shown that pollution sources of heavy metals in the environment mainly arise from anthropogenic sources. Portugal is a country with a long mining tradition. Land pollution due to mining activities is a major issue in many countries, and Portugal is not an exception (Candeias et al. 2014). In order to compare the Panasqueira regional soils with studies from other countries, where mining has been or still is a very important activity, several papers were selected from countries like Iran, China, Spain, South

Table 5 Comparison of heavy metal concentrations (mg kg^{-1}) observed in this study and those found in other heavy metal soil studies

Study location	As	Cd	Cu	Cr	Pb	Zn	References
Hunan Province (China)	na	0.2–11 (4)	22–170 (74)	23–55 (36)	17–74 (40)	91–485 (240)	Hu et al. (2014)
DraaLasfar Mine (Morocco)	9–3108	na	17–172	na	7–2309	30–1114	Pérez (2011)
Kettara Mine (Morocco)	10–237	na	27–1362	na	17–486	49–243	Pérez (2011)
Sidi-Bou Othmane Mine (Morocco)	10–112	na	25–46	na	23–6706	101–36,267	Pérez (2011)
Bir Nehass Mine (Morocco)	8–1113	na	24–46	na	19–1495	86–29,732	Pérez (2011)
Dexing (China)	2–52 (12)	0.04–2 (0.2)	6–629 (54)	99–659 (72)	16–244 (47)	27–799 (88)	Wu et al. (2014)
Dongguan (China)	1–128 (13)	0.02–2 (0.3)	7–2451 (67)	2–2434 (75)	4–9149 (160)	15–1674 (151)	Wu et al. (2015)
China (72 Mines)	(196)	(11)	(212)	(84)	(641)	(116)	Li et al. (2014)
Iran (3 Mines)	(146)	(2)	(88)	na	(1002)	(363)	Dayani and Mohammadi (2010) Rafiei et al. (2010)
Spain (16 Mines)	(192)	(7)	(121)	(63)	(882)	(466)	Rahimsouri et al. (2011) Li et al. (2014) Bueno et al. (2009) Chopin and Alloway (2007) Franco et al. (2006)
South Korea (70 Mines)	(70)	(2)	(79)	na	(111)	(183)	Kraus and Wiegand (2006) Lambrechts et al. (2011) Madejón et al. (2006) Martínez et al. (2007) Martínez López et al. (2008) Moreno-Jiménez et al. (2009) Navarro et al. (2008) Ordóñez et al. (2011) Oyarzun et al. (2009) Oyarzun et al. (2011) Rodríguez et al. (2009) Li et al. (2014)
Vietnam (3 mines)	(3144)	(135)	(271)	(1501)	(31)	(41)	Chon et al. (2011) Jung (2008) Kim et al. (2005) Kim et al. (2008) Ko et al. (2010) Lee et al. (2005) Lim et al. (2008) Li et al. (2014) Chu Ngoc et al. (2009) Ha et al. (2011)

Table 5 (continued)

Study location	As	Cd	Cu	Cr	Pb	Zn	References
India (5 Mines)	(19)	(4)	(64)	(1509)	(305)	(339)	Kien et al. (2010) Li et al. (2014) Anju and Banerjee (2012) Das and Chakrapani (2011) Krishna et al. (2010) Ladwani et al. (2012) Sadhu et al. (2012) Li et al. (2014)
China (21 urban soils)	(15)	(2)	(99)	(77)	(61)	(133)	Luo et al. (2012) Li et al. (2014)
China (12 agricultural soils)	(10)	(0.4)	(32)	(59)	(38)	(118)	Wei and Yang (2010) Li et al. (2014)
Portugal (652 soil samples)	1–226 (9)	na	1–245 (14)	1–336 (18)	2–585 (21)	5–738 (46)	Ferreira (2004)
Aljustrel Mine (Portugal)	1–3936 (99)	0.1–62 (0.6)	10–5414 (135)	6–115 (57)	13–20,000 (417)	22–20,000 (233)	Candeias et al. (2011a, b)
Lousal Mine (Portugal)	510–4436 (1051)	0.3–10 (2)	266–5578 (995)	na	1446–11,424 (4066)	164–5550 (1249)	Ferreira da Silva et al. (2005)
Argozelo Mine (Portugal)	4–8200 (526)	2–12 (2)	25–968 (132)	4–226 (91)	8–118 (18)	76–1006 (237)	Ávila and Santos Oliveira (2004)
Jales Mine (Portugal)	10–1308 (227)	1–23 (1)	10–82 (28)	5–609 (118)	23–592 (110)	68–277 (124)	Ávila and Santos Oliveira (2004)
Vale das Gatas Mine (Portugal)	1–226 (9)	1–226 (9)	1–245 (14)	1–336 (18)	2–585 (21)	5–738 (46)	Ávila and Santos Oliveira (2004)
Panasqueira Mine (Portugal)	17–1503 (102)	0.1–4 (4)	10–292 (42)	10–166 (7)	9–97 (2)	22–199 (77)	Present study
Mean world soils	5	0.3	25	80	17	70	Reimann and Caritat (1998)
Ontario soils reference values	11	1	62	67	45	290	Ministry of the Environment (2011)
Portuguese soils reference values	22	0.6	35	43	34	85	Ferreira (2004)

Data are presented as minimum, maximum, and mean values (min–max (mean)) and also reference values

na not available

Korea, Vietnam, and India and also other mine sites in Portugal, and the results were compiled (Table 5). It is possible to understand that the environment surrounding these mining areas is often polluted by heavy metals dispersed from the mining operations. From Table 5, the mean concentrations of all listed heavy metals are higher in many of these countries, and the Portuguese soils surrounding mining areas like Lousal, Argozelo, and Jales mines present mean values of As, Pb, and Zn higher than the mining areas in Iran, Spain, India, and South Korea. The soils surrounding Panasqueira mine also contain high concentrations in some of the listed elements, namely in As and Cd, being classified as contaminated soils. This finding reflects the significance of the mining activities in generating heavy metal pollution as well as the greater impact that mining has on soil pollution when compared with the baseline values.

Conclusions

The mining and beneficiation processes at Panasqueira mine produces arsenic-rich mine wastes responsible for the high levels of metals at the Barroca Grande and Rio tailings. Tailings and open-air impoundments are the main source of pollution in the surrounding area due to the sulfide oxidation that enhances the mobilization and migration of trace metals from the mining wastes into the environment. PCA results obtained for topsoils allowed the identification of Ag, As, Bi, Cd, Cu, W, and Zn association supporting the above sentence.

The estimated pollution load index (PLI) established a local soil quality classification through 100 % of topsoil samples with moderate to high degree of contamination. The PLI spatial distribution showed that soils are potential toxic elements (As, Cd, Cu, Pb, and Bi) enriched, when compared with local background soils. Selective chemical extraction prove that As, Cd, Cu, and Zn are linked to the exchangeable and acid-soluble bearing phases, upon which desorption and ion exchange reactions may originate the release of these readily mobile phases.

Based on the results of the pollution and risk assessment studies, the soils surrounding Panasqueira mining area are polluted by heavy metals emitted from the mining activity. Considering that high concentrations of potential toxic elements (e.g., Ag, Cd, Cu, As, Bi, and Zn) were observed in local soils and local populations are probably exposed to some potential health risks

through the inhalation and the ingestion of water and vegetables, some additional studies are required. The practical results of this study allow selecting areas where an eventual remediation procedure may be foreseen. Priority should be given to areas where samples are classified as requiring reclamation, when they are geographically located in agricultural or urban areas.

Acknowledgments This research is financially supported by Fundação para a Ciência e a Tecnologia (FCT) (grant SFRH/BD/63349/2009).

Conflict of interest The authors declare no conflict of interests.

References

- Abdi, H., & Williams, L. (2010). Principal component analysis. *Wiley Interdisciplinary Reviews: Computational Statistics*, 2(4), 433–459. doi:10.1002/wics.101.
- Akai, J., & Anawar, M. (2013). Mineralogical approach in elucidation of contamination mechanism for toxic trace elements in the environment: special reference to arsenic contamination in groundwater. *Physics and Chemistry of the Earth, Parts A/B/C*, 58–60, 2–12. doi:10.1016/j.pce.2013.04.011.
- Anju, M., & Banerjee, D. K. (2012). Multivariate statistical analysis of heavy metals in soils of a Pb–Zn mining area, India. *Environmental Monitoring and Assessment*, 184, 4191–4206.
- Ávila, P., Ferreira da Silva, E., Farinha, J. Á. (2008a). Geochemical distribution and behavior of Arsenic in the vicinity of the active Sn–W Panasqueira mine, Central Portugal. In *Int workshop GeochemArsenic* (pp. 2–7).
- Ávila, P. F., & Santos Oliveira, J. M. (2004). *Geochemistry of soils on the influence of some abandoned mines of the Trás-os-Montes region (Portugal)*. Bragança: I Iberian Congress of Soil Science.
- Ávila, P., Ferreira da Silva, E., Salgueiro, A. R., & Farinha, J. Á. (2008b). Geochemistry and mineralogy of mill tailings impoundments from the Panasqueira mine (Portugal): implications for the Surrounding Environment. *Journal of International Mine Water Association*, 27(3), 210–224.
- Bednar, A. J., Boyd, R. E., Jones, W. T., McGrath, C. J., Johnson, D. R., Chappell, M. A., & Ringelberg, D. B. (2009). Investigations of tungsten mobility in soil using column tests. *Chemosphere*, 75(8), 1049–1056.
- Bini, C., Sartori, G., Wahsha, M., & Fontana, S. (2011). Background levels of trace elements and soil geochemistry at regional level in NE Italy. *Journal of Geochemical Exploration*, 109(1–3), 125–133.
- Bloot, C., & de Wolf, L. C. M. (1953). Geological features of the Panasqueira tin-tungsten ore occurrence (Portugal). *Boletim de la Sociedad Geológica Portuguesa*, 11(1), 1–58.
- Breiter, K. (2001). Report about laboratory investigations of rock samples from the Panasqueira mine and recommendations for future exploration. *Panasqueira Mine not published Rep.*

- Bueno, P. C., Bellido, E., Rubí, J. A. M., & Ballesta, R. J. (2009). Concentration and spatial variability of mercury and other heavy metals in surface soil samples of periurban waste mine tailing along a transect in the Almadén mining district (Spain). *Environmental Geology*, *56*, 815–824.
- Candeias, C., Ferreira da Silva, E., Salgueiro, A., Pereira, H., Reis, A., Patinha, C., Matos, J., & Ávila, P. H. (2011a). The use of multivariate statistical analysis of geochemical data for assessing the spatial distribution of soil contamination by potentially toxic elements in the Aljustrel mining area (Iberian Pyrite Belt, Portugal). *Environmental Earth Sciences*, *62*, 1461–1479.
- Candeias, C., Ferreira da Silva, E., Salgueiro, A., Pereira, H., Reis, A., Patinha, C., Matos, J. X., & Ávila, P. H. (2011b). Assessment of the soil contamination by potentially toxic elements in Aljustrel mining area in order to implement soil reclamation strategies. *Land Degradation and Development*, *22*, 565–585.
- Candeias, C., Melo, R., Ávila, P. F., Ferreira da Silva, E., Salgueiro, A., & Teixeira, J. P. (2014). Heavy metal pollution in mine–soil–plant system in S. Francisco de Assis—Panasqueira mine (Portugal). *Applied Geochemistry*, *44*, 12–26.
- Cardoso, J. C., Bessa, M. T., Marado, M. B. (1971). Carta III.1 – Carta de solos 1:1 000 000, Atlas do Ambiente. *Instituto do Ambiente*, Lisboa (in Portuguese).
- Cavey, G., & Gunning, D. (2006). *Updated technical report on the Panasqueira mine, Castelo Branco District*. Portugal: OREQUEST.
- CD-ROM Atlas do Potencial Eólico para Portugal Continental – Version 1.0. Instituto Nacional de Engenharia, Tecnologia e Inovação (2004). ISBN 972-676-196-4 (in Portuguese).
- Cheng, H. X., Li, M., Zhao, C. D., Li, K., Peng, M., Qin, A. H., & Cheng, X. M. (2014). Overview of trace metals in the urban soil of 31 metropolises in China. *Journal of Geochemical Exploration*, *139*, 31–52.
- Chon, H. T., Lee, J. S., & Lee, J. U. (2011). Heavy metal contamination of soil, its risk assessment and bioremediation. *Geotechnical Engineering*, *14*, 191–206.
- Chopin, E. I. B., & Alloway, B. J. (2007). Distribution and mobility of trace elements in soils and vegetation around the mining and smelting areas of Tharsis, Riotinto and Huelva, Iberian Pyrite Belt, SW Spain. *Water, Air, and Soil Pollution*, *182*, 245–261.
- Chu Ngoc, K., Van Nguyen, N., Nguyen Dinh, B., Le Thanh, S., Tanaka, S., Kang, Y., et al. (2009). Arsenic and heavy metal concentrations in agricultural soils around tin and tungsten mines in the Dai Tu district, N. Vietnam. *Water, Air, and Soil Pollution*, *197*, 75–89.
- Costa, P. A. S. (2004). Atlas do potencial eólico para Portugal Continental. *MSc thesis, Sciences Fac, Lisbon Univ* (in Portuguese).
- Costa, P., Estanqueiro, A. (2006a). Development and validation of the Portuguese Wind Atlas. In *Proc Eur Wind Ener Conf*, (EWEC), Athens.
- Costa, P., Estanqueiro, A. (2006b). Building a Wind Atlas for mainland Portugal using a weather type classification. *Proc Eur Wind Energy Conf*, (EWEC), Athens.
- Das, S. K., & Chakrapani, G. J. (2011). Assessment of trace metal toxicity in soils of Raniganj Coalfield, India. *Environmental Monitoring and Assessment*, *177*, 63–71.
- Dayani, M., & Mohammadi, J. (2010). Geostatistical assessment of Pb, Zn and Cd contamination in near-surface soils of the urban-mining transitional region of Isfahan, Iran. *Pedosphere*, *20*, 568–577.
- Deschamps, E., Ciminelli, V. S. T., Lange, F. T., Matschullat, J., Raue, B., & Schmidt, H. (2002). Soil and sediment geochemistry of the Iron Quadrangle, Brazil: the case of arsenic. *Journal of Soils and Sediments*, *2*(4), 216–222.
- e-Ecorisk (2007). A regional enterprise network decision-support system for environmental risk and disaster management of large-scale industrial soils. Contract n.º EGV1-CT-2002-00068, WP3 – case study site characterization, *ProjManag Rep, Deliverable 3.1*.
- Fernandes-Caliani, J. C., Barba-Brioso, C., Gonzales, I., & Galán, E. (2009). Heavy metal pollution in soils around the abandoned mine sites of Iberian pyrite belt (Southwest Spain). *Water, Air, and Soil Pollution*, *200*, 211–226.
- Ferreira, M. M. S. I. (2004). Dados geoquímicos de base de solos de Portugal Continental, utilizando amostragem de baixa densidade. *PhD Thesis, Aveiro University* (in Portuguese).
- Ferreira da Silva, E., Cardoso Fonseca, E., Matos, J., Patinha, C., Reis, P., & Santos Oliveira, J. M. (2005). The effect of unconfined mine tailings on the geochemistry of soils, sediments and surface waters of the Lousal area (Iberian Pyrite Belt, Southern Portugal). *Land Degradation and Development*, *16*, 213–228.
- Ferreira da Silva, E., Ávila, P. F., Salgueiro, A., Candeias, C., & Pereira, H. (2013). Quantitative–spatial assessment of soil contamination in S. Francisco de Assis due to mining activity of the Panasqueira mine (Portugal). *Environmental Science and Pollution Research*, *20*(11), 7534–7549. doi:10.1007/s11356-013-1495-2.
- Fiedler, H. J., & Rösler, H. J. (1993). *Spurenelemente in der Umwelt*. Jena: Gustav Fischer Verlag (in dutch).
- Franco, C., Soares, A., & Delgado, J. (2006). Geostatistical modelling of heavy metal contamination in the topsoil of Guadiamar river margins (S Spain) using a stochastic simulation technique. *Geoderma*, *136*, 852–864.
- Garrigues, S., Allard, D., Barete, F., & Morissette, J. (2008). Multivariate quantification of landscape spatial heterogeneity using variogram models. *Remote Sensing of Environment*, *112*(1), 216–230.
- Ha, N. T. H., Sakakibara, M., Sano, S., & Nhuan, M. T. (2011). Uptake of metals and metalloids by plants growing in a lead–zinc mine area, Northern Vietnam. *Journal of Hazardous Materials*, *186*, 1384–1391.
- Hu, X. F., Jiang, Y., Shu, Y., Hu, X., Liu, L., & Luo, F. (2014). Effects of mining wastewater discharges on heavy metal pollution and soil enzyme activity of the paddy fields. *Journal of Geochemical Exploration*, *147*(B), 139–150.
- Jaques Ribeiro, L. M., & Gonçalves, A. C. R. (2013). Contributo para o conhecimento geológico e geomorfológico da área envolvente do Couto Mineiro da Panasqueira. Centro de Estudos de Geografia e Ordenamento do Território. *Geografia e Ordenamento do Território*, *3*, 93–116 (in Portuguese).
- Julivert, F., Fontboté, J., Ribeiro, A., Conde, L. (1974). Mapa Tectónico de la Península Ibérica y Baleares, escala 1:1, 000,000. *InstGeolMineroEspaña*, Madrid (in Spanish).

- Jung, M. C. (2008). Heavy metal concentrations in soils and factors affecting metal uptake by plants in the vicinity of a Korean Cu-W mine. *Sensors*, 8, 2413–2423.
- Kabata-Pendias, A. (2011). Trace elements in soils and plants. 4th ed. CRC press.
- Kabata-Pendias, A., Mukherjee, A. (2007). *Trace elements from soil to human*. Springer-Verlag.
- Karim, Z., Qureshi, B. A., & Mumtaz, M. (2015). Geochemical baseline determination and pollution assessment of heavy metals in urban soils of Karachi, Pakistan. *Ecological Indicators*, 48, 358–364.
- Kelly, W. C., & Rye, R. O. (1979). Geologic, fluid inclusion and stable isotope studies of the tin-tungsten deposits of Panasqueira, Portugal. *Economic Geology*, 74, 1721–1822.
- Kien, C. N., Noi, N. V., Son, L. T., Ngoc, H. M., Tanaka, S., Nishina, T., et al. (2010). Heavy metal contamination of agricultural soils around a chromite mine in Vietnam. *Soil Science Plant Nutrition*, 56, 344–356.
- Kim, J. Y., Kim, K. W., Ahn, J. S., Ko, I., & Lee, C. H. (2005). Investigation and risk assessment modeling of As and other heavy metals contamination around five abandoned metal mines in Korea. *Environmental Geochemistry and Health*, 27, 193–203.
- Kim, S., Kwon, H. J., Cheong, H. K., Choi, K., Jang, J. Y., Jeong, W. C., et al. (2008). Investigation on health effects of an abandoned metal mine. *Journal of Korean Medical Science*, 23, 452–458.
- Ko, B. G., Park, S. J., Jung, G. B., Kim, M. K., Kim, G. Y., Hong, S. Y., et al. (2010). Characteristics of soil heavy metal contents in the agricultural areas near closed mine in Korea. 19th World Congress of Soil Science, Soil Solutions for a Changing World, pp. 27–30.
- Kraus, U., & Wiegand, J. (2006). Long-term effects of the Aznalcollar mine spill—heavy metal content and mobility in soils and sediments of the Guadamar river valley (SW Spain). *The Science of the Total Environment*, 367, 855–871.
- Krishna, A.K., Mohan, K.R., Murthy, N.N. (2010). Heavy metal pollution in soils around the abandoned mine sites of Nuggihalli Schist Belt, Karnataka, India. *Geochimica et Cosmochimica Acta*, 74, A30.
- Ladwani, K. D., Ladwani, K. D., Manik, V. S., & Ramteke, D. S. (2012). Assessment of heavy metal contaminated soil near coal mining area in Gujarat by toxicity characteristics leaching procedure. *International Journal of Life Sciences Biotechnology and Pharma Research*, 1, 73–80.
- Lambrechts, T., Couder, E., Bernal, M. P., Faz, Á., Iserentant, A., & Lutts, S. (2011). Assessment of heavy metal bioavailability in contaminated soils from a former mining area (La Union, Spain) using a rhizospheric test. *Water, Air, and Soil Pollution*, 217, 333–346.
- Leal, M. V. (1945). *As Minas da Panasqueira: vida e história*. Portugália Editora (in Portuguese).
- Lee, J. S., Chon, H. T., & Kim, K. W. (2005). Human risk assessment of As, Cd, Cu and Zn in the abandoned metal mine site. *Environmental Geochemistry and Health*, 27, 185–191.
- Levitán, D., Schreiber, M. E., Seal, R. R., II, Bodnar, R. J., & Aylor, J. G., Jr. (2014). Developing protocols for geochemical baseline studies: an example from the Coles Hill uranium deposit, Virginia, USA. *Applied Geochemistry*, 43, 88–100.
- Li, Z., Ma, Z., van der Kuijp, T. J., Yuan, Z., & Huang, L. (2014). A review of soil heavy metal pollution from mines in China: pollution and health risk assessment. *The Science of the Total Environment*, 468–469, 843–853.
- Lim, H. S., Lee, J. S., Chon, H. T., & Sager, M. (2008). Heavy metal contamination and health risk assessment in the vicinity of the abandoned Songcheon Au–Ag mine in Korea. *Journal of Geochemical Exploration*, 96, 223–230.
- Lotze, F. (1945). Observations respect a la division de los variscides de la Meseta Ibérica. *Publ Estrag Geol*, 5, 149–166 (in Spanish).
- Luo, X. S., Yu, S., Zhu, Y. G., & Li, X. D. (2012). Trace metal contamination in urban soils of China. *The Science of the Total Environment*, 421–422, 17–30.
- Madejón, P., Murillo, J. M., Marañón, T., Espinar, J. L., & Cabrera, F. (2006). Accumulation of As, Cd and selected trace elements in tubers of *Scirpusmaritimus* L. from Doñana marshes (South Spain). *Chemosphere*, 64, 742–748.
- Martínez López, J., Llamas Borrajo, J., de Miguel García, E., Rey Arrans, J., Hidalgo Estévez, M. C., & Sáez Castillo, A. (2008). Multivariate analysis of contamination in the mining district of Linares (Jaén, Spain). *Applied Geochemistry*, 23, 2324–2336.
- Martínez, J., Llamas, J., De Miguel, E., Rey, J., & Hidalgo, M. C. (2007). Determination of the geochemical background in a metal mining site: example of the mining district of Linares (South Spain). *Journal of Geochemical Exploration*, 94, 19–29.
- Mench, M. (1993). Notions sur les éléments en traces pour une qualité des sols et des produits végétaux. *Purpan*, 166, 118–127 (in French).
- Ministry of the Environment. (2011). *Soil, groundwater and sediment standards for the use under Part XV.1 of the environmental protection act*. Ontario: E-Publishing.
- Moncur, M. C., Jambor, J. L., Ptacek, C. J., & Blowes, D. W. (2009). Mine drainage from the weathering of sulfide minerals and magnetite. *Applied Geochemistry*, 24, 2362–2373.
- Moreno-Jiménez, E., Peñalosa, J. M., Manzano, R., Carpena-Ruiz, R. O., Gamarra, R., & Esteban, E. (2009). Heavy metals distribution in soils surrounding an abandoned mine in NW Madrid (Spain) and their transference to wild flora. *Journal of Hazardous Materials*, 162, 854–859.
- Navarro, M. C., Pérez-Sirvent, C., Martínez-Sánchez, M. J., Vidal, J., Tovar, P. J., & Bech, J. (2008). Abandoned mine sites as a source of contamination by heavy metals: a case study in a semi-arid zone. *Journal of Geochemical Exploration*, 96, 183–193.
- Noronha, F., Doria, A., Dubessy, J., & Charoy, B. (1992). Characterization and timing of the different types of fluids present in the barren and ore veins of the W-Sn deposit of Panasqueira, Central Portugal. *Mineral Deposits*, 27, 72–79.
- Ordóñez, A., Álvarez, R., Charlesworth, S., De Miguel, E., & Loredom, J. (2011). Risk assessment of soils contaminated by mercury mining, Northern Spain. *Journal of Environmental Monitoring*, 13, 128–136.
- Oyarzun, R., Cubas, P., Higuera, P., Lillo, J., & Llanos, W. (2009). Environmental assessment of the arsenic-rich, Rodalquilar gold–(copper–lead–zinc) mining district, SE Spain: data from soils and vegetation. *Environmental Geology*, 58, 761–777.
- Oyarzun, R., Lillo, J., López-García, J. A., Esbrí, J. M., Cubas, P., Llanos, W., et al. (2011). The Mazarrón Pb–(Ag)–Zn mining district (SE Spain) as a source of heavy metal contamination

- in a semiarid realm: geochemical data from mine wastes, soils, and stream sediments. *Journal of Geochemical Exploration*, 109, 113–124.
- Pérez, M. A. (2011). Studies of polluted mine soils and treatment of wastewaters. Applications of synchrotron based techniques, field portable XRay Fluorescence and advanced oxidation processes. PhD thesis, 207 pp.
- Polya, D. A. (1989). Chemistry of the main stage ore-forming fluids of the Panasqueira W-Cu(Ag)-Sn deposit, Portugal: implications for models of ore genesis. *Economic Geology*, 84, 1134–1152.
- Radojevic, M., & Bashkin, V. N. (1999). *Practical environmental analysis*. Cambridge: Royal Soc Chem.
- Rafiei, B., Khodaei, A. S., Khodabakhsh, S., Hashemi, M., & Nejad, M. B. (2010). Contamination assessment of lead, zinc, copper, cadmium, arsenic and antimony in Ahangaran mine soils, Malayer, West of Iran. *Soil and Sediment Contamination: An International Journal*, 19, 15.
- Rahimsouri, Y., Yaghubpur, A., Modabberi, S., & Alipour, S. (2011). Environmental impacts of natural contaminants and mining activities on the surface and agricultural soils in the Aq-Darreh river watershed, Takab, West Azerbaijan Province, NW Iran. *Iranian Journal of Science and Technology*, 2, 101–111.
- Reimann, C., & Caritat, P. (1998). *Chemical elements in the environment: factsheets for the geochemist and environmental scientist*. Berlin: Springer Verlag.
- Reis, A. C. (1971). As Minas da Panasqueira. *Bol Minas*, 8(1), 3–34 (in Portuguese).
- Rodríguez, L., Ruiz, E., Alonso-Azcárate, J., & Rincón, J. (2009). Heavy metal distribution and chemical speciation in tailings and soils around a Pb-Zn mine in Spain. *Journal of Environmental Management*, 90, 1106–1116.
- Sadhu, K., Adhikari, K., & Gangopadhyay, A. (2012). Assessment of heavy metal contamination of soils in and around open cast mines of Raniganj area, India. *International Journal of Environmental Engineering*, 1, 77–85.
- Son, H., & Jung, M. C. (2011). Relative extraction ratio (RER) for arsenic and heavy metals in soils and tailings from various metal mines, Korea. *Environmental Geochemistry and Health*. doi:10.1007/s10653-010-9356-0.
- Sousa, B. (1985). Perspectiva sobre os conhecimentos actuais do Complexo Xisto-Grauváquico de Portugal. *Mem Not Mus Lab Min Geol Univ Coimbra*, 100, 1–16 (in Portuguese).
- Thadeu, D. (1951). Geologia do couro mineiro da Panasqueira. *Comunicações dos Serviços Geológicos de Portugal*, 32, 5–64 (in Portuguese).
- Violante, A., Cozzolino, V., Perelomov, L., Caporale, A. G., & Pigna, M. (2010). Mobility and bioavailability of heavy metals and metalloids in soil environments. *Journal of Soil Science and Plant Nutrition*, 10(3), 268–292.
- Wei, B. G., & Yang, L. S. (2010). A review of heavy metal contaminations in urban soils, urban road dusts and agricultural soils from China. *Microchemical Journal*, 94, 99–107.
- Wimmers, D. (1983). *Sulfide mineralogy of the wolframite-bearing veins on level 2, Barroca Grande, Panasqueira, Portugal*. Int rept. Free University Amsterdam.
- Wu, J., Teng, Y., Lu, S., Wang, Y., & Jiao, X. (2014). Evaluation of soil contamination indices in a mining area of Jiangxi, China. *PLoS ONE*, 9(11), e112917. doi:10.1371/journal.pone.0112917.
- Wu, S., Peng, S., Zhang, X., Wu, D., Luo, W., Zhang, T., Zhou, S., Yang, G., Wan, H., & Wu, L. (2015). Levels and health risk assessments of heavy metals in urban soils in Dongguan, China. *Journal of Geochemical Exploration*, 148, 71–78.
- Xie, X.-D., Min, X.-B., Chai, L.-Y., Tang, C.-J., Liang, Y.-J., Li, M., Ke, Y., Chen, J., & Wang, Y. (2013). Quantitative evaluation of environmental risks of flotation tailings from hydrothermal sulfidation–flotation process. *Environmental Science and Pollution Research*, 20, 6050–6058.
- Zhang, C., Quiao, Q., Piper, J. D., & Huang, B. (2011). Assessment of heavy metal pollution from a Fe-smelting plant in urban river sediments using environmental magnetic and geochemical methods. *Environmental Pollution*, 159, 3057–3070.